EDGEWOOD CHEMICAL BIOLOGICAL CENTER
U.S. ARMY RESEARCH, DEVELOPMENT AND ENGINEERING COMMAND
Aberdeen Proving Ground, MD 21010-5424

ECBC-TR-957

METAL ION-CATALYZED ALCOHOLYSIS AS A STRATEGY FOR THE DESTRUCTION OF ORGANOPHOSPHORUS CHEMICAL WARFARE AGENTS

H. Dupont Durst
Frederic J. Berg

RESEARCH AND TECHNOLOGY DIRECTORATE

R. Stanley Brown
Alexei A. Neverov
Andrea Tamer

QUEEN'S UNIVERSITY
Kingston, Ontario, Canada K7l 3N6

July 2018

U.S. ARMY RDECOM

Disclaimer

The findings in this report are not to be construed as an official Department of the Army position unless so designated by other authorizing documents.

REPORT DOCUMENTATION PAGE

Form Approved
OMB No. 0704-0188

1. REPORT DATE *(DD-MM-YYYY)*	2. REPORT TYPE	3. DATES COVERED *(From - To)*
XX-07-2018	Final	Aug 2009 – Nov 2010

4. TITLE AND SUBTITLE
Metal Ion-Catalyzed Alcoholysis as a Strategy for the Destruction of Organophosphorus Chemical Warfare Agents

5a. CONTRACT NUMBER
DHS IAA No. HSHQDC-09-X-00543

5b. GRANT NUMBER

5c. PROGRAM ELEMENT NUMBER

6. AUTHOR(S)
Durst, H. Dupont*; Berg, Frederic J. (ECBC); Brown, R. Stanley; Neverov, Alexei A.; and Tamer, Andrea (Queen's University);

5d. PROJECT NUMBER

5e. TASK NUMBER

5f. WORK UNIT NUMBER

7. PERFORMING ORGANIZATION NAME(S) AND ADDRESS(ES)
Director, ECBC, ATTN: RDCB-DRC-C, APG, MD 21010-5424
Department of Chemistry, Chernoff Hall, 90 Bader Lane, Queen's University, Kingston, Ontario, Canada K7L 3N6

8. PERFORMING ORGANIZATION REPORT NUMBER
ECBC-TR-957

9. SPONSORING / MONITORING AGENCY NAME(S) AND ADDRESS(ES)
U.S. Department of Homeland Security, ATTN: Homeland Security Advanced Research Projects Agency, Building 410, 245 Murray Lane SW, Washington, DC 20528-0001

10. SPONSOR/MONITOR'S ACRONYM(S)
HSARPA

11. SPONSOR/MONITOR'S REPORT NUMBER(S)

12. DISTRIBUTION / AVAILABILITY STATEMENT
Approved for public release: distribution unlimited.

13. SUPPLEMENTARY NOTES
* H. Dupont Durst retired from ECBC.

14. ABSTRACT-LIMIT 200 WORDS

Metal ion-catalyzed alcoholysis has proven to be an effective strategy for the rapid transformation of neutral reactive organophosphate esters of the phosphate, phosphonate, phosphorothioate, and phosphonothioate classes. This chemistry, using $La^{3+}(^{-}OMe)$/methanol as a catalyst or solvent, which was applied to the V- and G-classes of chemical warfare agents, demonstrated extremely rapid transformation to low toxicity esters with load factors up to ~30% for nonfluoride-releasing agents. Variation of the alcohol solvent is tolerated. Variations of the metal catalyst provide potential redress to the fluoride inhibition of the class of G-agents. These observations indicate that formulations based on mixed alcohol solvents, combined with optimized metal catalysts for use in field decontamination, civilian security, and infrastructure scenarios, provide a pathway for "tuning" the reaction media while retaining rapid destruction kinetics.

15. SUBJECT TERMS
Metal ion-catalyzed alcoholysis (MICA)
G- and V-nerve agents
31 Phosphorus nuclear magnetic resonance (^{31}P NMR)
Decontamination
Pesticide
Organophosphorus (OP)

16. SECURITY CLASSIFICATION OF:			17. LIMITATION OF ABSTRACT	18. NUMBER OF PAGES	19a. NAME OF RESPONSIBLE PERSON
a. REPORT	b. ABSTRACT	c. THIS PAGE			Renu B. Rastogi
U	U	U	UU	52	19b. TELEPHONE NUMBER *(include area code)* (410) 436-7545

Blank

PREFACE

The work described in this report was authorized under U.S. Department of Homeland Security Interagency Agreement contract number HSHQDC-09-X-00543. The work was started in August 2009 and completed in November 2010.

The use of either trade or manufacturers' names in this report does not constitute an official endorsement of any commercial products. The report may not be cited for purposes of advertisement.

This report has been approved for public release.

Blank

EXECUTIVE SUMMARY

Metal ion-catalyzed alcoholysis has proven to be an effective strategy for the rapid transformation of neutral reactive organophosphate esters of the phosphate, phosphonate, phosphorothioate, and phosphonothioate classes. This chemistry uses $La^{3+}(^{-}OMe)$/methanol as a catalyst or solvent. When applied to the V- and G-classes of chemical weapons agents, this chemistry demonstrated extremely rapid transformation to low toxicity esters with load factors of ~30% for nonfluoride-releasing agents. Variation of the alcohol solvent indicated that ethanol and ethanolamine are equally effective in this system. Synthetic chemistry was developed to rapidly provide independent standards of the diester products for unambiguous product assignment. In addition, variations of the metal catalyst provided potential redress to the fluoride inhibition of the G-agent class. These observations indicated that formulations, which are based on mixed alcohol solvents, combined with optimized metal catalysts for use in field decontamination, civilian security, and infrastructure scenarios, provide a pathway for "tuning" the reaction media and retaining rapid destruction kinetics.

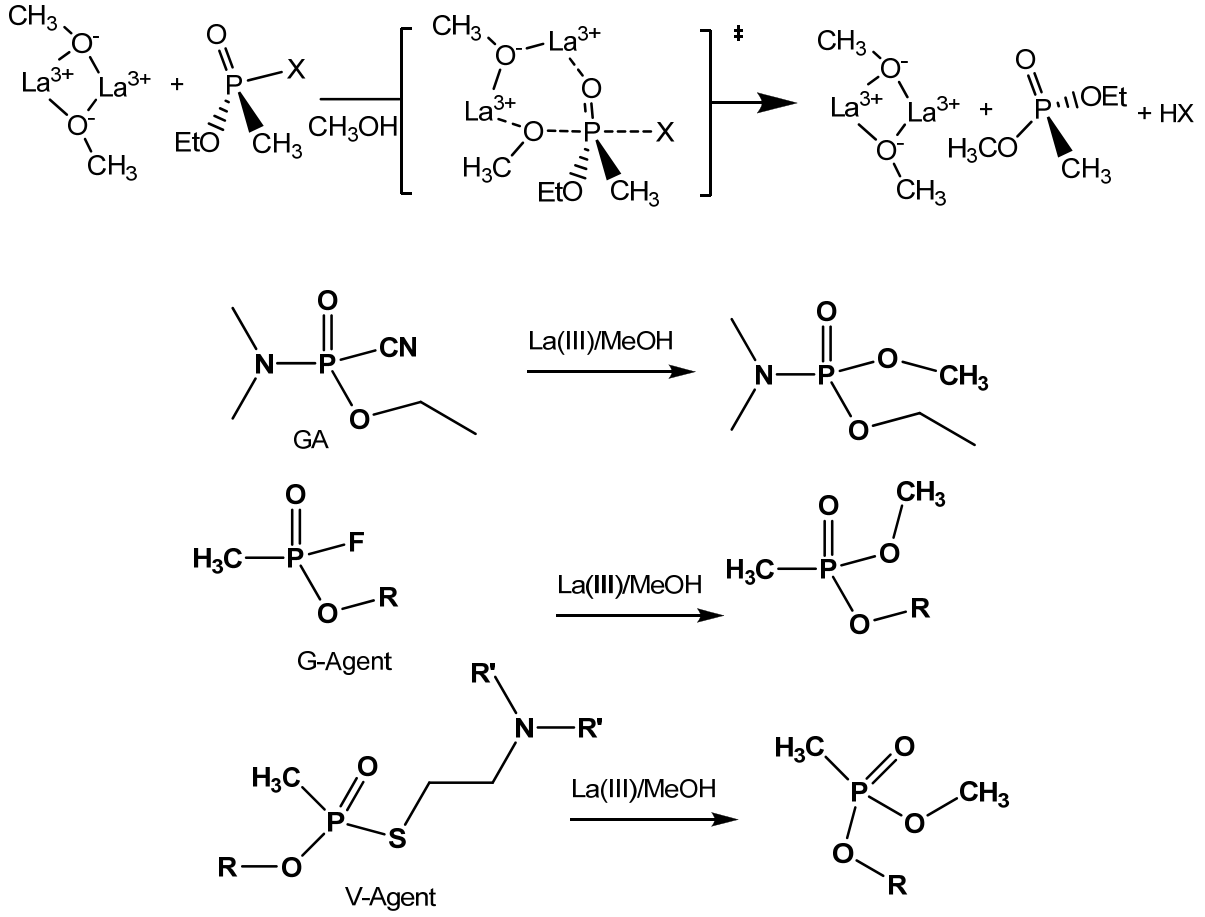

Graphical abstract: Overview of reaction mechanism with specific examples of products resulting from GA (tabun; a fluoride-releasing G-agent) and a V-agent.

Blank

CONTENTS

FIGURES

TABLES

METAL ION-CATALYZED ALCOHOLYSIS AS A STRATEGY FOR THE DESTRUCTION OF ORGANOPHOSPHORUS CHEMICAL WARFARE AGENTS

1. INTRODUCTION

Activated organophosphate, phosphinate, and phosphonate esters are potent acetylcholinesterase inhibitors that are used as animal and crop protectants and chemical warfare agents (CWAs). Whether these inhibitors are used as pesticides or CWAs, all act in the same manner by inhibiting an a cholinesterase enzyme. They interfere with normal neurotransmission, which ultimately leads to respiratory failure and death. The use of organophosphorus (OP) pesticides, such as malathion, diazinon, cygon (dimethoate), and other easily available materials, is widespread, and most of these can be purchased in an unrestricted fashion. Recent estimates by the U.S. Environmental Protection Agency indicate that in the United States, 73 million pounds of the active ingredients for these inhibitors are used annually. Estimates of quantities used throughout the world are about 10 times this amount or 365,000 tons per year. Despite the beneficial uses of these inhibitors, increasing concern exists regarding soil and water contamination arising from spills and improper use. At the same time, pesticide demands are increasing to sustain worldwide food demand. Consequently, it is highly unlikely that use of these inhibitors will be eliminated in the near future.

Recent geopolitical events have focused much attention on OP CWAs. Developed and widely stockpiled as defensive measures by several countries after World War II, these materials no longer have any legitimate purposes other than as deterrents of first-strike use by potential adversaries. Concerns are increasing that these materials, whether home-synthesized or pilfered from stockpiled or found sources, could become the preferred weapons of terrorist organizations. In an effort to rid the world of these materials, the 1992 Chemical Weapons Convention (CWC) Treaty[1] required total destruction of scheduled stockpiles of chemical weapons by the signatory nations. (By 2012, membership to the CWC included 192 nations that represented over 97% of the world population.)

Given the abundance and lethality of OP chemical weapons and the increasing possibility of terrorist activities, considerable research is being performed to create methods for facilitating the controlled decomposition of these materials.[2–6] Although good methods are prevalent for the decomposition of several of these materials, many of these methods have deficiencies, and no single technique is appropriate for all types of chemical weapons. Therefore, an urgent need exists for new, rapid, and effective decontamination methodologies.

2. ADVANTAGES OF METAL ION-CATALYZED ALCOHOLYSIS (MICA) OVER HYDROLYSIS

MICA reactions for the inactivation of reactive OP esters have been studied for many years.[7–9] These are relatively well-understood processes, in which the reactions typically involve catalytically active $M^{x+}(^{-}OR)$ species. The metal ion plays several roles, such as the following:

- decreasing the acid dissociation constant (pKa) of the metal-associated HOR so that an $M^{x+}(^{-}OR)$ can be formed at or near neutral pH;
- creating a bifunctional role, in which the $M^{x+}(^{-}OR)$ acts as a Lewis acid, coordinating transiently to the P=O group, which allows a subsequent intramolecular delivery of the coordinated alkoxide; and
- possibly promoting an accelerated breakdown of any intermediates through coordination of the leaving group (particularly a poor one) with the metal ion.

Water is required as a reagent for hydrolytic processes; however, there are significant disadvantages associated with using it as a reaction medium for metal-catalyzed reactions. Although the $M^{x+}(^{-}OH)$ species are catalytically active, they generally form oligomeric and polymeric gels or precipitates that are poorly soluble in aqueous media, which complicates mechanistic analyses, particularly at a higher pH. By contrast, their alkoxide analogs ($M^{x+}(^{-}OR)$) are soluble, even at relatively high concentrations in alcohol at high pH; therefore, detailed studies of MICA reactions of carboxylate and phosphate esters are possible.[5] Perhaps, more importantly, M^{x+} hydroxides in water are not particularly reactive intermolecular catalysts for phosphoryl or acyl transfer reactions, and with rare exception, they are generally less reactive than free hydroxide for these processes. This might be expected for a system in which stabilizing a coordinated hydroxide by binding it to an electropositive metal ion should decrease its basicity and nucleophilicity. In such cases, the catalytic role of the metal ion is limited to providing a sufficient concentration of nucleophile (coordinated hydroxyanion) at lower pH values. However, we have found that M^{x+}-coordinated alkoxides in alcohol solvents are good nucleophiles for neutral phosphates and carboxylate esters with activities that are generally much higher than those for free alkoxide. Yang[5] reported that there is a synergistic role between low polarity, reduced dielectric constant alcohol solvents, and metal-coordinated alkoxides that leads to high reactivity of these systems. This probably includes several factors, such as increasing the transient ion–dipole binding of the metal complex and substrate and decreasing the activation energy for the reaction of the bound substrate–metal complex through a lower-polarity-solvent effect that favors transition states, in which charge is dispersed in comparison with the ground state.

Although phosphate triesters are not naturally occurring molecules and, therefore, have no known natural biological function, nature produces a class of phosphotriesterase (PTE) enzymes that are very effective at destroying neutral OP pesticides. Thus, organisms are protected from being poisoned by these materials. The two most studied PTEs (from *Agrobacterium radiobacter* and *Pseudomonas diminuta*) are dinuclear Zn(II) enzymes that have nearly 90% amino acid homology and conserve all the metal-binding ligands.[10] Although not exactly established, the mechanism of action for these enzymes has been discussed as involving intramolecular delivery of a Zn(II)-coordinated hydroxide (possibly one bridged between the two Zn(II) ions) to a neutral phosphate ester substrate that is activated by P=O coordination to the second Zn(II) ion.[11,12] This sort of dinuclear core is characteristic of other enzymes that mediate the hydrolytic cleavage of phosphate diesters[13–18] and monoesters.[19] In addition, it gives the *P. diminuta* bacterium the ability to hydrolytically decompose paraoxon (**1**), its preferred substrate, with a rate constant (k_{cat}) near the diffusion limit, $k_{cat}/K_m \sim 10^8$ mol^{-1} mL s^{-1} (where K_m is the Michaelis constant).[20] It is important to note that PTE enzymes also react with OP

chemical weapons, which suggests that enzyme-based systems or enzymes mimicking these detoxifying systems may be useful for decontamination.

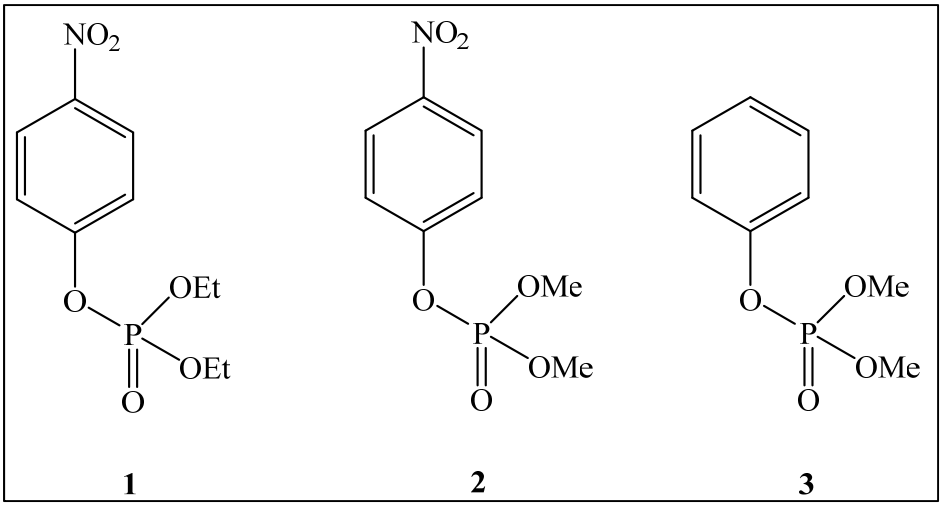

Figure 1. Structures of paraoxon (**1**), methyl paraoxon (**2**), and dimethyl phenyl phosphate (**3**).

Our strategy for developing an artificial PTE was based on the idea of a metal-coordinated nucleophile in a reduced-polarity medium that has a greater interaction with substrates with better reactivity than is possible with water. Cleland et al.[21] have suggested that "enzyme-active sites are nonaqueous, and the effective dielectric constants resemble those in organic solvents rather than those in water." Given that the dielectric constants of water, methanol, and ethanol are 78, 32.7, and 24.6, respectively, the light alcohols were chosen as the mediums for mimicking the reduced-polarity environment that is assumed to exist for the PTE enzymes.

3. EFFECTS OF METAL ION CATALYSIS OF PHOSPHORYL TRANSFER IN METHANOL MEDIUM

Our original experiments investigating the MICA of phosphate esters involved the methanolysis of the pesticide paraoxon (**1**) promoted by La^{3+} in methanol.[22] As shown in Figure 2, plots of the observed first-order rate constant (k_{obs}) as opposed to lanthanum trifluoromethanesulfonate ($La(OTf)_3$) concentration at three different negative logarithm of pH values in methanol (designated as ${}^{s}_{s}pH$)[5,12] are linear at higher La^{3+} concentrations with an upward curvature at lower concentrations. The upward curvature of the plot at lower La^{3+} concentrations indicates that the reaction is second-order in the La^{3+} concentration. The slopes of the linear sections of the graphs at higher La^{3+} concentrations are ${}^{s}_{s}pH$ dependent and are defined as the observed second-order rate constant (k_2^{obs}) values for the $(La^{3+})_2$-catalyzed reaction. Figure 3 shows a plot of log k_2^{obs} in relation with the ${}^{s}_{s}pH$ profile for the $(La^{3+})_2$-catalyzed reaction, which shows a distorted bell-shaped profile that plateaus between ${}^{s}_{s}pH$ values of 8 and 10.5.

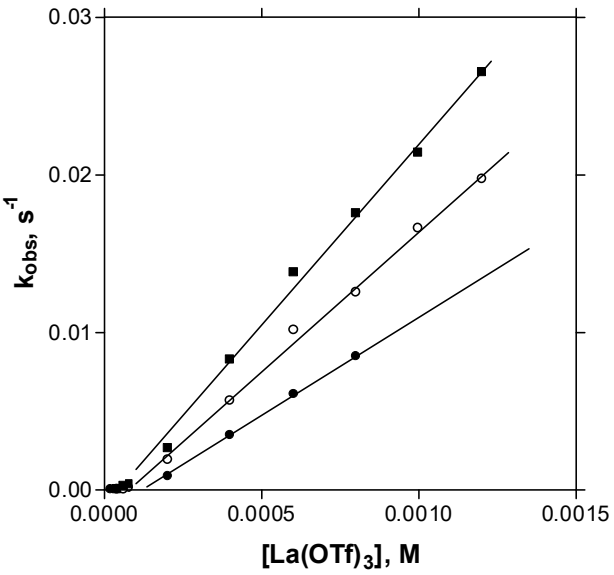

Figure 2. Plot of k_{obs} vs $La(OTf)_3$ for the La^{3+}-catalyzed methanolysis of paraoxon (**1**) (2.04×10^{-5} mol dm^{-3}) at 25 °C for ${}^{s}_{s}pH$ values of 8.96 (■), 8.23 (○), and 7.72 (•). (Reproduced with permission from Tsang et al.[22])

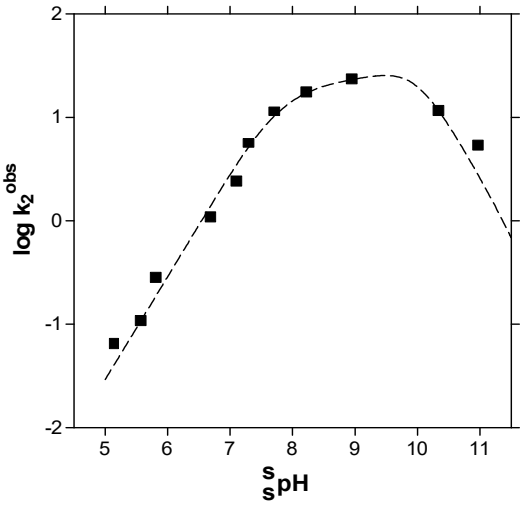

Figure 3. Plot of log second-order rate constant (k_2) vs ${}^{s}_{s}pH$ for La^{3+}-catalyzed methanolysis of paraoxon (**1**) at 25 °C. (Reproduced with permission from Tsang et al.[22])

The reactions in the plateau region are very fast, and they can be calculated from the k_2^{obs} values at ${}^{s}_{s}\mathrm{pH}$ 8.3–8.4 (neutral ${}^{s}_{s}\mathrm{pH}$ in methanol). A 2 mmol solution of La^{3+} (1 mmol/mL in $(La^{3+})_2$) has a half-life ($t_{1/2}$) of 20 s for the destruction of paraoxon (**1**). This corresponds to a 10^9-fold acceleration as opposed to the background reaction under the same conditions (the uncatalyzed $t_{1/2}$ is reported to be ~600 years at a near neutral ${}^{s}_{s}\mathrm{pH}$ of 8.3).[12] Further analysis involving potentiometric titrations of La^{3+} in methanol[7,23] indicated that the dimeric species responsible for catalysis had increasing numbers of associated methoxides at higher ${}^{s}_{s}\mathrm{pH}$ values (species represented as $(La^{3+})_2(^{-}OCH_3)_n$, where n assumes the values of 1–5). A detailed analysis of the data yielded the speciation diagram of $La^{3+}{}_2(^{-}OCH_3)_n$ complexes under the experimental conditions presented in Figure 4. These are shown together with the overlaid k_2^{obs} kinetics data to indicate that the dominant catalytically active species is $(La^{3+})_2(^{-}OCH_3)_2$ operating at a ${}^{s}_{s}\mathrm{pH}$ of ~9.

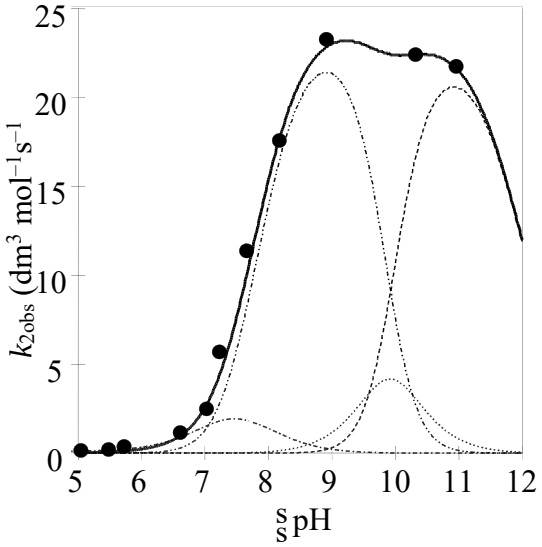

Figure 4. Plot of the predicted k_2^{obs} vs ${}^{s}_{s}\mathrm{pH}$ rate profile for La^{3+}-catalyzed methanolysis of paraoxon (**1**) (solid line) based on the kinetics contributions of (left to right) $La^{3+}{}_2(^{-}OCH_3)_1$, $La^{3+}{}_2(^{-}OCH_3)_2$, $La^{3+}{}_2(^{-}OCH_3)_3$, and $La^{3+}{}_2(^{-}OCH_3)_4$ computed from the $k_2^{2:1}$, $k_2^{2:2}$, $k_2^{2:3}$, and $k_2^{2:4}$ rate constants (Table 1) and their speciation as a function of ${}^{s}_{s}\mathrm{pH}$. (Reproduced with permission from Gibson et al.[23])

When the kinetics and speciation data were fitted to eq 1, individual second-order rate constants for each of the $(La^{3+})_2(^{-}OCH_3)_n$ species ($k_2^{2:n}$) were determined. These values are presented in Table 1.

$$k_2^{obs} = \{k_2^{2:1}[La^{3+}{}_2(^{-}OR)_1] + k_2^{2:2}[La^{3+}{}_2(^{-}OR)_2] + k_2^{2:n}[La^{3+}{}_2(^{-}OR)_n]\}/[La(OTf)_3]_t \qquad (1)$$

Table 1. Computed Second-Order Rate Constants ($k_2^{2:n}$) for the $(La^{3+})_2(^{-}OCH_3)_n$-Catalyzed Methanolysis of Paraoxon (**1**) Obtained through Fits of k_2^{obs} at Each $^{s}_{s}$pH by Eq 1

$(La^{3+})_2(^{-}OCH_3)_n$ Species	$k_2^{2:n}$ ($mmol^{-1}\ s^{-1}$)
$^{-}OCH_3$	$k_{OCH_3} = 0.011$
$(La^{3+})_2(^{-}OCH_3)_1$	$k_2^{2:1} = 15.8 \pm 2.9$
$(La^{3+})_2(^{-}OCH_3)_2$	$k_2^{2:2} = 51.1 \pm 1.1$
$(La^{3+})_2(^{-}OCH_3)_3$	$k_2^{2:3} = 35.6 \pm 6.5$
$(La^{3+})_2(^{-}OCH_3)_4$	$k_2^{2:4} = 49.7 \pm 1.4$

Notes: (1) Errors were computed from average percent deviations in fitted numbers calculated by eq 1 from actual kinetics data.
(2) Data are in part from Tsang et al. (high $^{s}_{s}$pH)[22] and Gibson et al.[23]

The activation parameters presented in Table 2 were determined for the $^{-}OCH_3$- and La^{3+}-catalyzed methanolysis of methyl paraoxon (**2**) and its parent compound, dimethyl phenyl phosphate (**3**). Although the enthalpies and entropies of activation for the base-catalyzed processes were as expected for this type of reaction, the La^{3+}-catalyzed processes had unusually low activation parameters. These values were consistent with the mechanism that proceeds through the formation of a transient complex between the catalyst and the substrate, followed by an "intramolecular" delivery of the metal ion-coordinated nucleophile to a substrate that is activated by Lewis acid coordination to the La^{3+} center. In such a case, the overall enthalpy of activation can be separated into two parts. The first part arises from the interaction between the catalyst and the substrate, and the second part relates to the actual "chemical" step. The expected negative value of the first component partially compensates for the expected small, but positive, enthalpy of activation, which is characteristic of an intramolecular Lewis acid promoted nucleophilic attack. The overall enthalpy was close to zero in the case of **2**. In the case of the slightly less electrophilic parent ester **3**, the second part should have shown a slightly higher positive enthalpy of activation, which would have been consistent with the values given in Table 2. The low change in enthalpy ($\Delta H^{\ddagger}$) that resulted from the complex-promoted cleavage of the bound substrates was achieved at the price of a large negative entropy, as would be expected for a highly ordered transition state involving association of two species with severely restricted degrees of freedom. Nevertheless, the low $\Delta H^{\ddagger}$ value means that the reactions were not very temperature dependent. Reducing the temperature from 25 to –25 °C only reduced the reaction rate by factors of 1.27 and 3 for substrates **2** and **3,** respectively.

Table 2. Activation Parameters for the Base- and La^{3+}-Catalyzed Methanolysis of Methyl Paraoxon (**2**) and Dimethyl Phenyl Phosphate (**3**)

Substrate	Term	Catalyst	
		CH_3O^-	$(La^{3+})_2$
2	$\Delta H^{\ddagger}$ (kJ mol^{-1})	61.6	3.14
	$\Delta S^{\ddagger}$ (J K^{-1} mol^{-1})	–67	–194.7
	$\Delta G^{\ddagger}$(25 °C) (kJ mol^{-1})	81.7	61.1
3	$\Delta H^{\ddagger}$ (kJ mol^{-1})	65.3	13.8
	$\Delta S^{\ddagger}$ (J K^{-1} mol^{-1})	–72.9	–183
	$\Delta G^{\ddagger}$ (25 °C) (kJ mol^{-1})	87	72.4

CH_3O^-: methoxide ion.
$\Delta S^{\ddagger}$: change in entropy.
$\Delta G^{\ddagger}$: change in Gibbs free energy.

4. METHANOLYSIS OF PHOSPHOROTHIOATES, PHOSPHONATES, AND PHOSPHONOTHIOATES

We investigated the metal ion-promoted methanolysis of other organophophorus compounds, such as dimethyl phenyl phosphate (**3**),[24] dimethyl aryl phosphorothioate (**4**),[25] and ethyl aryl methylphosphonothiate (**5**),[26] in the presence of La^{3+}, **6a**:Zn^{2+}($^-OCH_3$), and **6b**:Cu^{2+}($^-OCH_3$) (Figure 5). The reactions were studied at $^{s}_{s}pH$ values that generated the maximum rates for the metal-catalyzed reaction, which generally results when the complexes are formulated with one equivalent of methoxide for each metal ion present. For La^{3+}, the reaction $^{s}_{s}pH$ was set at 9.1 using an *N*-ethylmorpholine buffer, in which the dominant species was $(La^{3+})_2(^-OCH_3)_2$, whereas for **6a:**Zn^{2+}($^-OCH_3$) and **6b:**Cu^{2+}($^-OCH_3$), the operational $^{s}_{s}pH$ was set through half-neutralization of the complexes at 9.3 and 8.75,[27] respectively. The k_2 values for the $(La^{3+})_2(^-OCH_3)_2$-catalyzed reactions were once again defined as the slopes of the plots of the pseudo k_{obs} values as opposed to the catalyst concentrations. In the case of the **6a**:Zn^{2+}($^-OCH_3$) and **6b**:Cu^{2+}($^-OCH_3$) reactions, the k_2 values were twice the values of the gradients of these plots because setting the $^{s}_{s}pH$ by half-neutralization of the complexes produced only half of the active species. Based on those values, we calculated the expected $t_{1/2}$ values for the methanolysis of various substrates catalyzed by 1 mmol/mL of the active complex at 25 °C (Table 3).

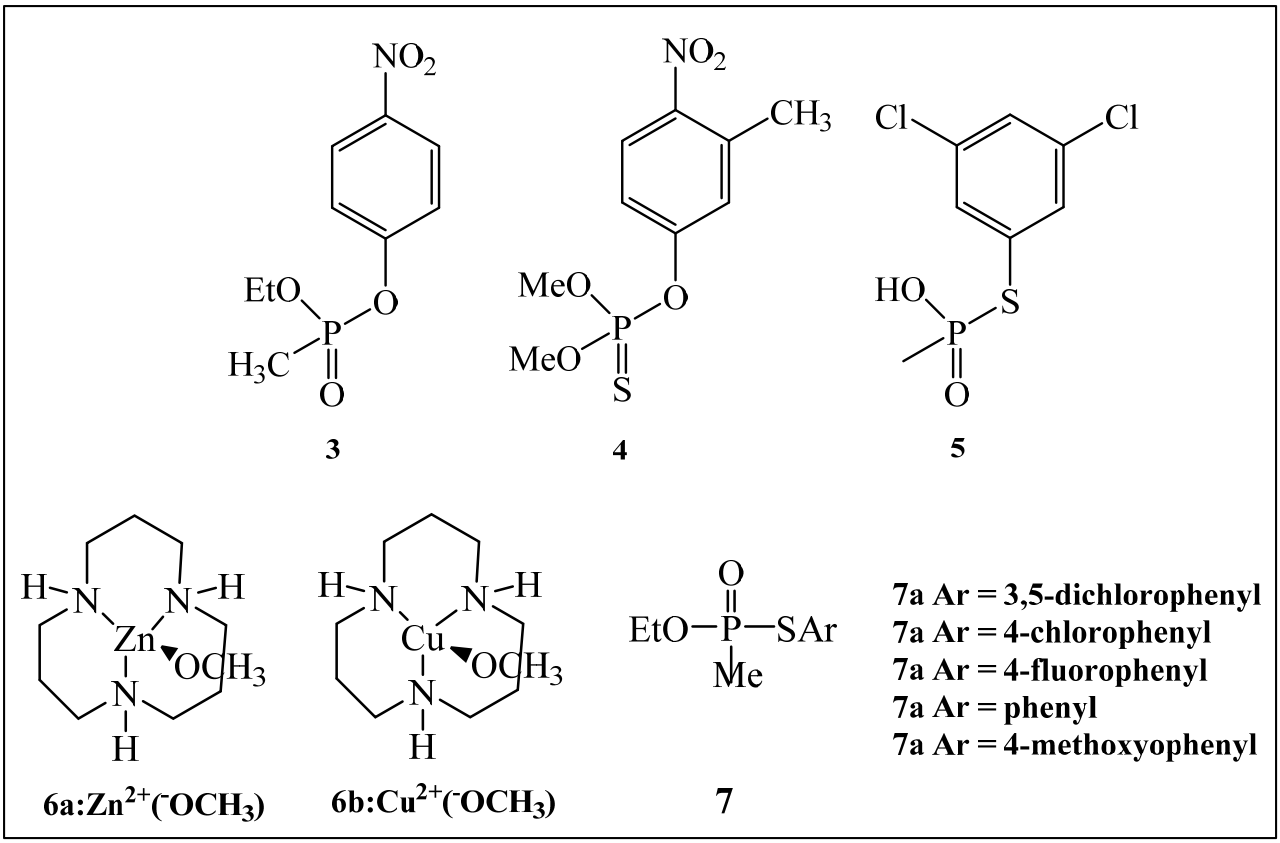

Figure 5. Structures of dimethyl phenyl phosphate (**3**), dimethyl aryl phosphorothioate (**4**), ethyl aryl methylphosphonothiate (**5**), **6a**:$Zn^{2+}(^{-}OCH_3)$, **6b**:$Cu^{2+}(^{-}OCH_3)$, and *S*-aryl methylphosphonothioates (**7a–e**).

Table 3. Expected $t_{1/2}$ Times for the Methanolysis of Organophosphates **3**, **4**, and **5** Catalyzed by a 1 mmol/mL Solution of Various Metal Ion Complexes at 25 °C

Catalyst	$t_{1/2}$ (s)		
	3	**4**	**5**
$La^{3+}{}_2(^{-}OCH_3)_2$	0.55	NR	0.14
6b:$Cu^{2+}(^{-}OCH_3)$	2.9	58	—
6a:$Zn^{2+}(^{-}OCH_3)$	15	1027	7.4

NR: no reaction.
—: data not available.

To predict the reactivity of metal complexes toward the U.S. *O*-ethyl-*S*-(2-diisopropylaminoethyl) methylphosphonothioate (USVX; Chemical Abstracts Service [CAS] number 50782-69-4) (**8**) (Figure 6), we prepared a series of substituted *S*-aryl methylphosphonothioates (**7a–e**) as simulants that structurally resemble this agent. Figure 7 shows three Brønsted plots of log $k_2^{catalyst}$ as opposed to the negative logarithm of the equilibrium constant for association ($^{s}_{s}pK_a$) of aryl thiol for the methanolysis of the series **7a–e** catalyzed by $(La^{3+})_2(^{-}OCH_3)$, **6a**:$Zn^{2+}(^{-}OCH_3)$, and methoxide anion, in which the respective slopes of the linear plots are $\beta = -0.75 \pm 0.01$, $\beta = -0.66 \pm 0.04$, and $\beta = -0.65 \pm 0.10$.

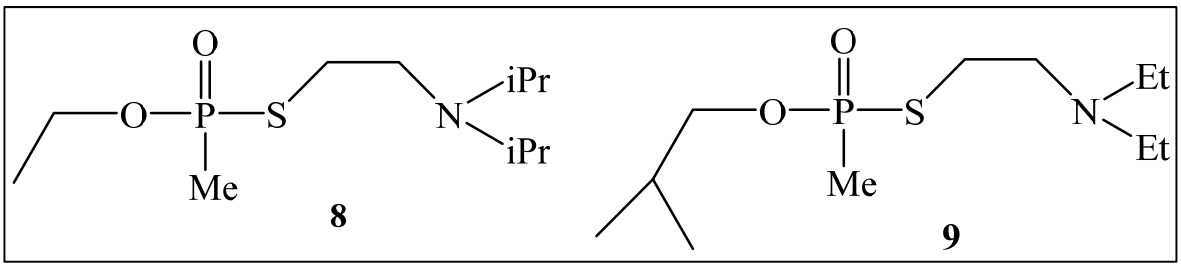

Figure 6. Structures of U.S. (**8**) and Russian (**9**) V-agents.

We independently determined a $^{s}_{s}pK_a$ of 9.54 for the ionization of the SH group of (*N*,*N*-diethylamino)ethanethiol (a thiol that resembles the leaving group of VX) in methanol. When placed on the various Brønsted plots, this $^{s}_{s}pK_a$ value yields predicted second-order rate constants for the reaction of VX promoted by the three nucleophiles. Accordingly, a 1 mmol/mL solution of **6a**:$Zn^{2+}(^{-}OCH_3)$ or $(La^{3+})_2(^{-}OCH_3)_2$ is predicted to decompose VX with half-times of 18 and 0.33 s.[16]

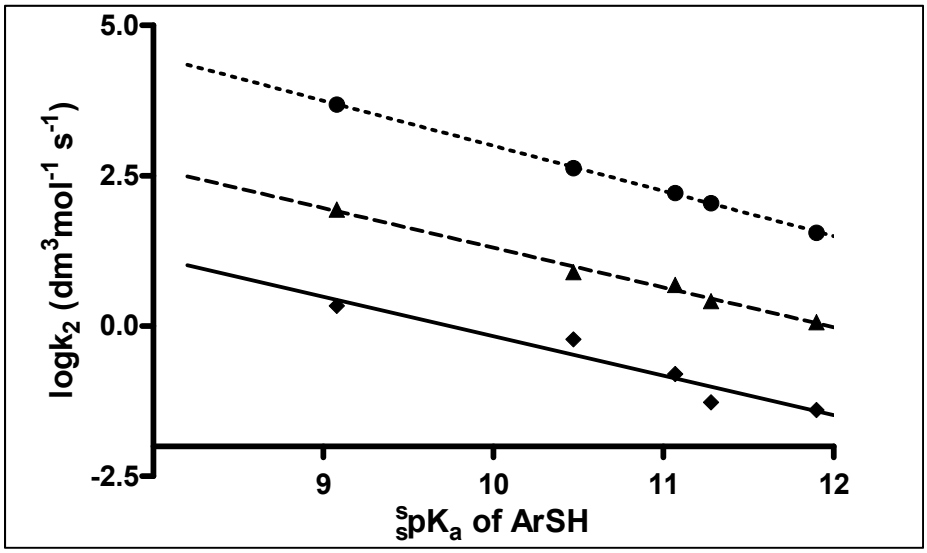

Figure 7. Brønsted plots for log $k_2^{catalyst}$ vs $^{s}_{s}pK_a$ of aryl thiol with $(La^{3+}(^{-}OCH_3))_2$ (●), **6a**:$Zn^{2+}(^{-}OCH_3)$ (▲), and $^{-}OCH_3$ (♦). (Reproduced with permission from Melnychuk et al.)[26]

5. TRANSESTERIFICATION IN CWA DECONTAMINATION BACKGROUND

Although not widely recognized, the use of transesterification as a basis for the destruction of CWAs has a rich history. A brief summary is provided for review.

5.1 Decontamination Solution 2 (DS2)

This organic solution, fielded by the U.S. Army in the early 1960s, consists of 2-methoxyethanol (methyl cellosolve), diethylenetriamine, and sodium hydroxide in a ratio of 28:70:2 wt %. Although initially thought to be a very effective hydroxide-based solution, a mechanistic study published in 1992 by Beaudry et al.[28] demonstrated that the hydroxide reacts with 2-methoxyethanol to produce the alkoxide form of this alcohol, and that with phosphorus-based CWAs, this is the nucleophile responsible for the chemistry. This solution is also deactivated by the addition of water in such a way that the reaction must be as organic as possible for the chemistry to be effective. This solution has low capacity and is stoichiometric, very caustic, and fast acting. This sequence is represented below in Figure 8.

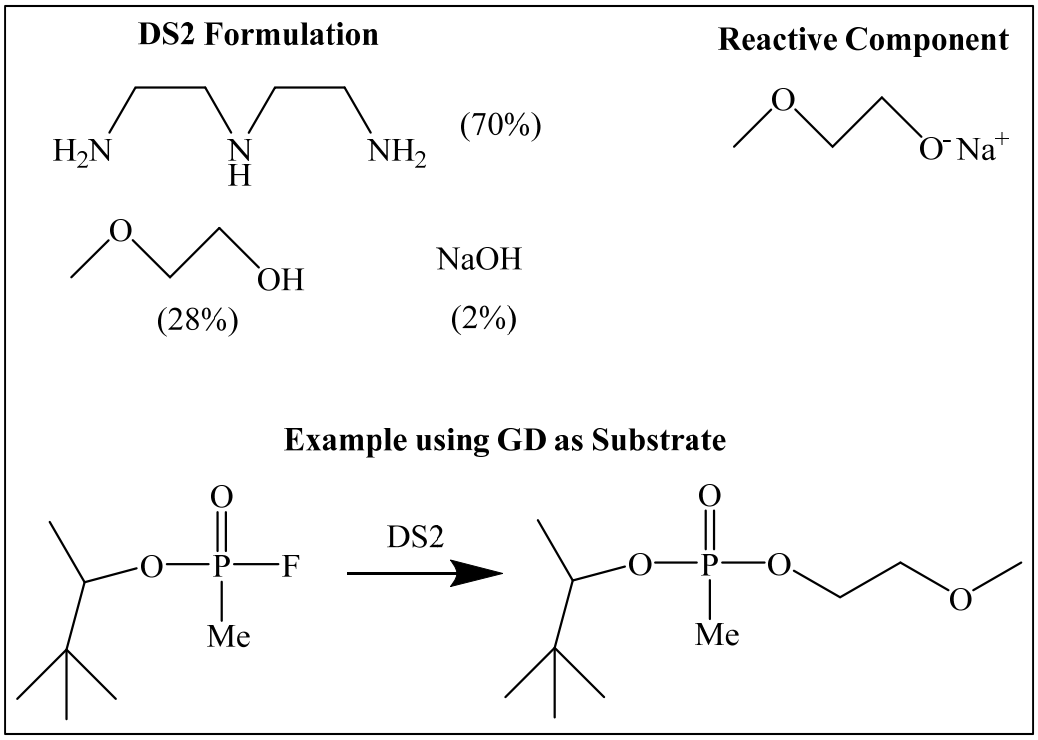

Figure 8. DS2 components and reaction example.

5.2 Russian Reactive Decontaminant 4, Modified (RD4M)

In 1994 and 1995, RD4M chemistry was extensively studied through the Russian–American Joint Evaluation Program[29–31] (RAJEP) at U.S. Army Edgewood Chemical Biological Center (ECBC; Aberdeen Proving Ground, MD) and Saratov (Saratov Oblast, Russian

Federation). The solution consists of potassium isobutylate in isobutyl alcohol. This reagent was demonstrated to be effective against soman (GD) and Russian *O*-(2-methylpropyl)-*S*-(2-diethylaminoethyl) methylphosphonothioate (RVX; CAS no. 159939-87-4) (**9**), with the mechanism being transesterification at phosphorus. Although it is expensive and slightly dangerous to make using classical synthetic methods (i.e., materials are potassium metal and anhydrous isobutanol), RD4M was effectively produced by a proprietary process developed by the State Research Institute of Organic Chemistry and Technology (GosNIIOKhT; Moscow, Russia) using potassium hydroxide as the base source. After a demonstration of the chemistry from the RAJEP program, this reagent was approved for use in the Russian chemical weapon demilitarization program. This solution has high capacity, and it is stoichiometric, very caustic, and fast acting. The reaction sequence is shown in Figure 9.

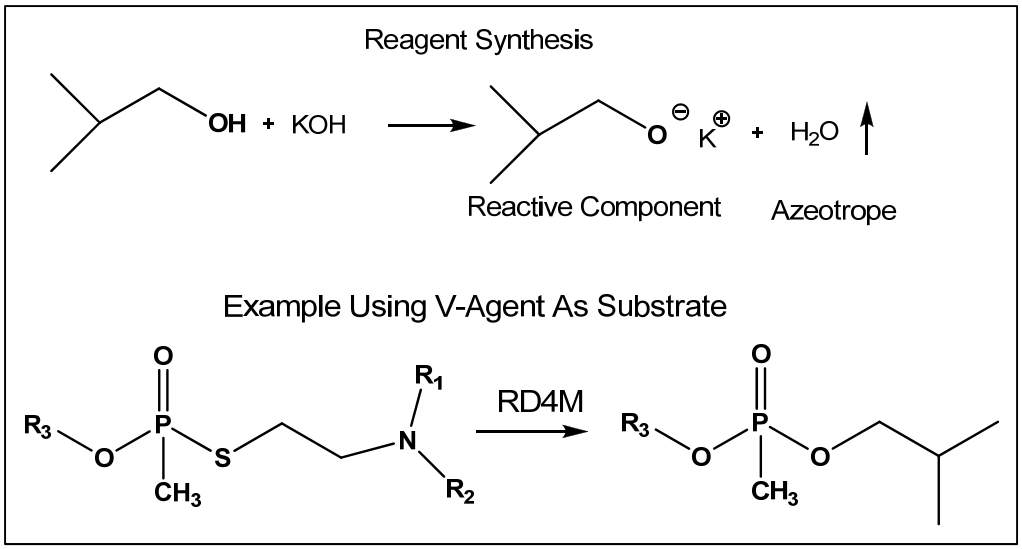

Figure 9. RD4M components and reaction example.

5.3 Ethanolamine: U.S. Nonstockpile Decontamination Solution

In 1997, based on experience gained with the RD4M system, ECBC personnel developed a reagent comprised of ethanolamine and potassium hydroxide.[32–36] This solution was very effective against V-type compounds. Mechanistic studies indicated that, like DS2, the active component in the mixture was the alkoxide and not the hydroxide of ethanolamine. This solution had very high capacity and was caustic, fast acting, and stoichiometric. This chemistry is illustrated in Figure 10.

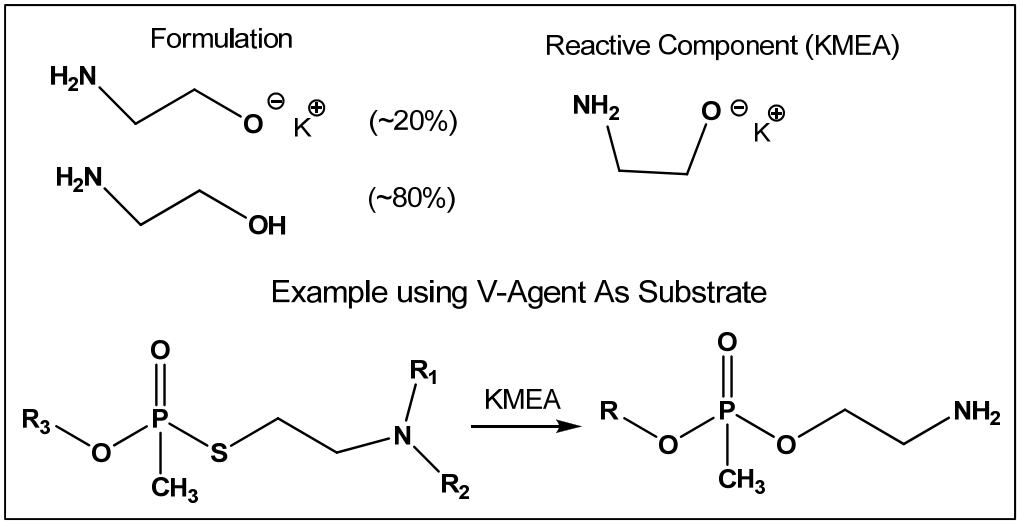

Figure 10. U.S. nonstockpile decontamination solution components and reaction example.

5.4 DS2, RD4M, and Ethanolamine: Advantages and Disadvantages

In all three examples, the reaction kinetics were very fast acting, and the production of EA 2192 was suppressed (unlike the chemistry associated with aqueous hydroxide or bleach-based systems). However, all of these are caustic (DS2 is a particularly corrosive solution) and stoichiometric. Material compatibility is also a significant issue with these systems.

6. EXPERIMENTAL METHODS

6.1 Simulant for G-Agents Developed at ECBC

We used an effective simulant for V-agents that was developed at ECBC. This simulant yielded good correlation between V-agents in range-finding studies. We used an inexpensive starting material, *P,P*-dichlorophenylphosphine; the general synthesis of this material is based on the work of DeBruin et al.,[37] which was used to prepare the USVX and RVX simulants (Figure 11).

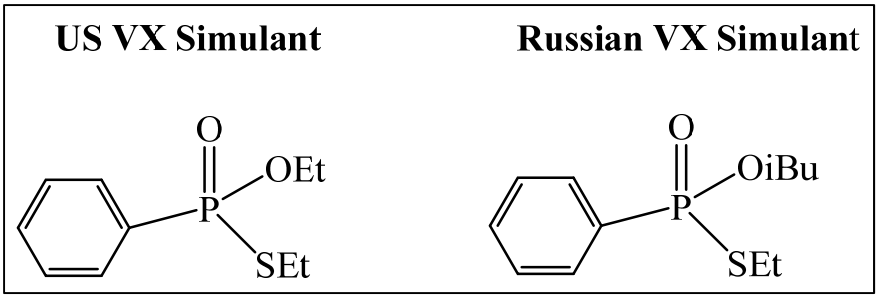

Figure 11. Structures of VX simulants.

A literature review was performed to determine the toxicity of the USVX simulant and whether exposure to this material leads to OP ester-induced delayed neuropathy (OPIDN or delayed neurotoxicity). OPIDN is characterized by flaccid paralysis of the extremities accompanied by axonal degeneration. OPIDN can occur after a single exposure or multiple dose exposures to OP compounds having the structure and activity requirements necessary to generate the delayed neurotoxicity. In experiments to study the delayed neurotoxicity of the USVX simulant in hens, no OPIDN symptoms were exhibited.[38] In additional studies of this class of compounds, no delayed neurotoxic effects were indicated.[39] Based on these results, this class of simulants is not considered to be delayed neurotoxicants. In the acute toxicity data for this compound,[40] the oral dose that is lethal to 50% of test subjects (the LD_{50} value) is 75 mg/kg for rats, which is considered only mildly toxic. This contrasts with the methylphosphonic acid equivalent ester, *O,S*-diethyl methylphosphonothioate (EA 5533), for which an oral LD_{50} of 3.7 mg/kg for rats was determined.[41] This class of compounds has been documented in several studies as simulants for V-type agents.[42–46] A similar compound for G-agents has not been described.

Chemistry was developed using diester alkylphosphonate, which, when reacted with thionyl chloride in the presence of a catalytic amount of dimethylformamide, led to the production of mono-ester phosphonochloridate as the only product. Application of this chemistry to di-*n*-butyl-*n*-butylphosphonate cleanly yielded *n*-butyl-*n*-butylphosphonochloridate. This chemistry (developed at ECBC), together with a simple reaction of properly prepared NaF, converted the chloro-compound into the G-analog *n*-butyl-*n*-butylphosphonoflouridate in high yields using a simple synthetic workup (Figure 12).

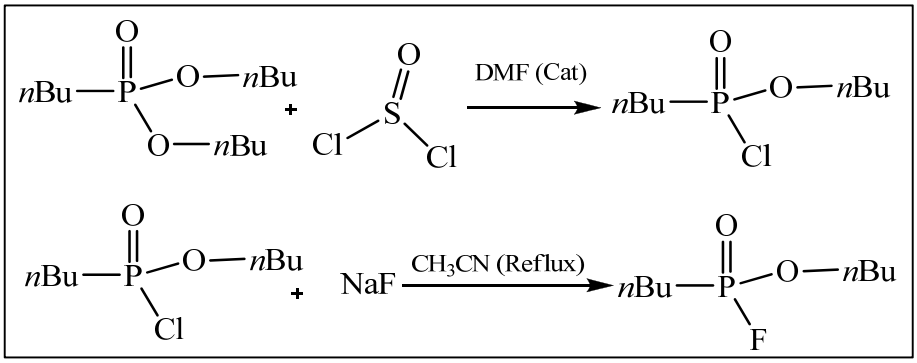

Figure 12. Synthesis of G-agent simulants.

To our knowledge, this derivative of the G-agent class has not been reported in the open literature. The advantages of both simulants are (1) they are not controlled by the treaty, nor are they defined as surety agents by the Army; (2) they require inexpensive, commercially available reagents; and (3) the toxicity of alkylphosphonofloridates, in which the alkyl group is not methyl, ethyl, propyl, or isopropyl, is much lower than those with that structure. The reaction and physical properties chemistries are very close to those of cyclosarin (GF) and GD agents.

Toxicology testing is being planned, and the results will be included in a separate technical report.

6.2 Synthesis of Product Standards

During the evaluation of different variations of solvent systems, a standard procedure for the synthesis of the expected products was developed. At the core of the strategy was the use of the thionyl chloride reaction (Figure 12) for the synthesis of the G-agent simulant. The synthesis diverges at the chloridate stage, in which, instead of conversion to the fluoride derivative, conversion to the mixed ester is accomplished. This strategy begins with relatively inexpensive, commercially available starting materials and allows multiple product variations to be obtained with essentially the same synthetic procedure. A specific example of this general transformation is the conversion of diisopropyl methylphosphonate (DIMP) into methyl isopropyl methylphosphonate through the intermediate chloridate, which is the expected product from sarin (GB) (Figure 13).

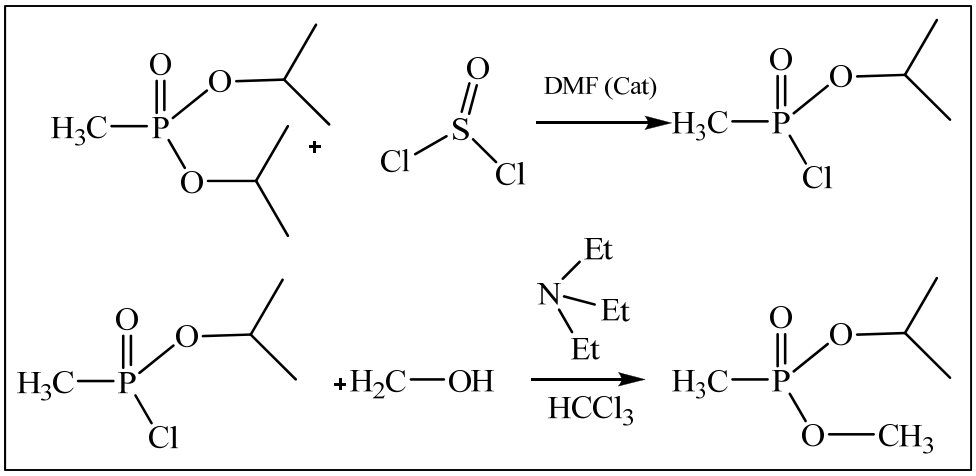

Figure 13. Formation of GB-reaction product.

6.3 Synthesis of Model EA 2192 Compounds

All the anionic derivatives of phosphonothioates (**7a–e**) were prepared by the following general route from methylphosphonic dichloride through *S*,*S*′-diarylmethylphosphonothioate. Thiophenol (10 mM) was added to a solution of methylphosphonic dichloride (5 mM) in dry dichloromethane, and triethylamine (10 mM) was slowly added to the mixture. The reaction mixture was stirred at 40 °C for 4 h. After the solvent was removed under reduced pressure, the residue was dissolved in 15 mL dichloromethane. The dichloromethane solution was washed with water (6 × 15 mL), and the combined aqueous layers were extracted with dichloromethane (3 × 15 mL). The combined organic layers were washed with saturated aqueous sodium chloride (10 mL) and dried over anhydrous sodium sulfate, and the resulting isolated product was *S*,*S*′-diarylmethylphosphonothioate (90% yield). The *S*,*S*′-diarylmethylphosphonothioate solution was then added to a mixture of 5M aqueous potassium hydroxide (3 mL) and dioxane (16 mL) and stirred at 50 °C for 8 h. The solution was

concentrated under reduced pressure to remove dioxane. To remove the thiol from the aqueous layer, the pH was brought down to 6–7, and the thiol was extracted with dichloromethane. The aqueous layer was then acidified with 3M aqueous hydrogen chloride (20 mL), and the acidic solution was extracted with dichloromethane (3 × 15 mL). The combined extracts were washed with saturated aqueous sodium chloride (10 mL) and dried over anhydrous sodium sulfate. Dichloromethane was removed under reduced pressure, and the isolated product was pure acid phosphonothioate in ≥80% yield.

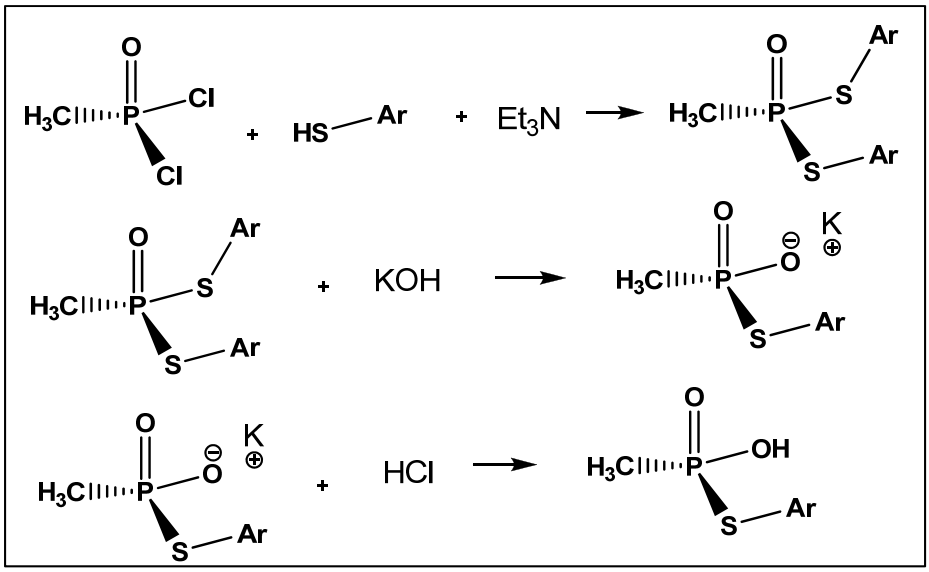

Figure 14. Synthesis of EA 2192 model compounds.

6.4 Ethanolamine/La^{3+}-Mediated Decomposition of Phosphonate Substrates

6.4.1 Materials

Ethanolamine (purified grade; Fisher Scientific; Pittsburg, PA), $La(OTf)_3$, tetrabutylammonium fluoride ($(Bu_4N^+)F^-$), and samarium trifluoromethansulfonate ($Sm(OTf)_3$) were purchased from Sigma-Aldrich. Lanthanum methanesulfonate ($La(OMs)_3$) was purchased from Chemical and Technical Developments Ltd. (Salisbury, Wilts, U.K.).

6.4.2 Kinetics Study

Stock solutions of 50 mM $La(OTf)_3$, $La(Ms)_3$, and $Sm(OTf)_3$ were prepared in ethanolamine; sodium ethoxide (50 mM) was prepared in anhydrous ethanol; a stock solution of 150 mM $(Bu_4N^+)F^-$ was prepared in ethanolamine; and stock solutions (10 mM) of *p*-nitrophenyl ethyl methylphosphonate and paraoxon were prepared in acetonitrile. Kinetics studies were performed by ultraviolet–visible (UV-vis) spectrophotometry, and the kinetics of the appearance of the *p*-nitrophenoxide product was monitored at 25 °C and 385 nm under pseudo-first-order conditions of excess catalyst. In each experiment, the final volume was 2.5 mL.

In the first set of kinetics experiments, either 1, 2, 3, or 5 mM of $La(X)_3$ (where X = OTf, OMs) was prepared in 70% ethanolamine with either 30% ethanol (v/v) or 30% methanol (v/v), and the kinetics of decomposition of *p*-nitrophenyl ethyl methylphosphonate were monitored. The results are shown in Tables 5–7. The effects of water and fluoride were studied using 5 mM $La(OTf)_3$ in ethanolamine, ethanolamine with 30% ethanol, and ethanolamine with 30% methanol, and the kinetics of decomposition of *p*-nitrophenyl ethyl methylphosphonate were monitored. The results are shown in Tables 8 and 9.
The effects of water on the decomposition of *p*-nitrophenyl ethyl methylphosphonate were studied using 5 mM $Sm(OTf)_3$ in ethanolamine and ethanolamine with 30% methanol. The results are shown in Table 10. The effects of complex aging on $La(OTf)_3$ and $Sm(OTf)_3$ (5 mM) with 20% water present for periods up to 24 h were studied by measuring the rate constant for the reaction with *p*-nitrophenyl ethyl methylphosphonate after 0 min to 24 h of aging in ethanolamine and in ethanolamine with 30% ethanol. The results are shown in Tables 11 and 12.

The behavior of solutions containing high concentrations of $La(OTf)_3$ (100, 50, and 30 mM) and $Sm(OTf)_3$ (50 mM) in ethanolamine and in ethanolamine with 30% ethanol were assessed by measuring their effects on the rate constant for decomposition of paraoxon and *p*-nitrophenyl ethyl methylphosphonate in the presence of variable amounts of water. The results are shown in Tables 13–16.

6.5 CWA Experimental Design

6.5.1 Reaction Criteria

There are two standard, generally recognized criteria for testing the destruction efficiency of reagents upon CWAs. The first is the North Atlantic Treaty Organization (NATO) standard, in which the ratio of agent-to-decontamination sample load is set at 1:100 (v/v). The second is common in U.S. testing, whereby the agent-to-decontamination sample load is set at 1:50 (v/v). In addition, an in-house addition to the 1:50 ratio is used at ECBC, so that the minimum rate for destruction kinetics should be 10 half-lives in 10 min at room temperature.

6.5.2 "Force-to-Fail" Criteria

In addition to the common reaction criteria, as discussed in Section 6.5.1, another set of criteria, called force to fail, was developed at ECBC in the mid-1980s. The experimental sequence in force to fail starts as a "load–load" agent-to-decontamination solution (1:100; 1:50). The agent load is increased in separate multiple additions, and the reaction progress is monitored. The force-to-fail point is the point at which the chemistry shuts down and significant quantities of residual agent remain after addition.

6.5.3 Experimental Design

Virtually all of the evaluations at ECBC were performed using phosphorus-31 nuclear magnetic resonance spectroscopy (^{31}P NMR) techniques on a JEOL ECX-400

spectrometer operating at 161.83 MHz, fitted with an ASC8 Auto Sample Changer (JEOL, Ltd.; Peabody, MA). All measurements were performed at 22 °C. Baseline resonance frequencies for neat agent in methanol were measured before each series at the 2.5% load. To evaluate force-to-fail criteria at low neat agent concentrations (<~8%), neat agent was measured into a nuclear magnetic resonance (NMR) tube, and a set volume of decontamination reagent was added. The sample was mixed by shaking and then immediately placed in the spectrometer. The total time lapse between mixing and first results was ~4 min. Continued interrogation of the sample was performed every 2 min until either no agent peak was observed or the 10 min time limit had been reached. To evaluate force-to-fail criteria at higher neat agent concentrations (>~8%), the neat agent was first weighed and then put in a 4 mL vial. In a separate 4 mL vial, the appropriate decontamination solution was measured. The decontamination solution was added to the agent vial, and the contents were mixed before being added to an NMR tube. NMR measurements were performed in the same manner as described for the low concentration evaluation.

7. RESULTS

7.1 Hydrolysis versus Transesterification: EA 2192 Problem

MICA is a lanthanide/methanol-based decontamination solution that exhibits extremely high activity for the decomposition of OP CWAs, such as G- and V-agents. However, samples of V-agents, particularly ones subjected to weathering, can contain products of partial V-agent hydrolysis, namely, EA 2192 ($^{-}OP(CH_3)(=O)(SR)$). In addition, EA 2192 can be formed during decontamination procedures that include hydrolytic methodologies, as shown in Figure 15.

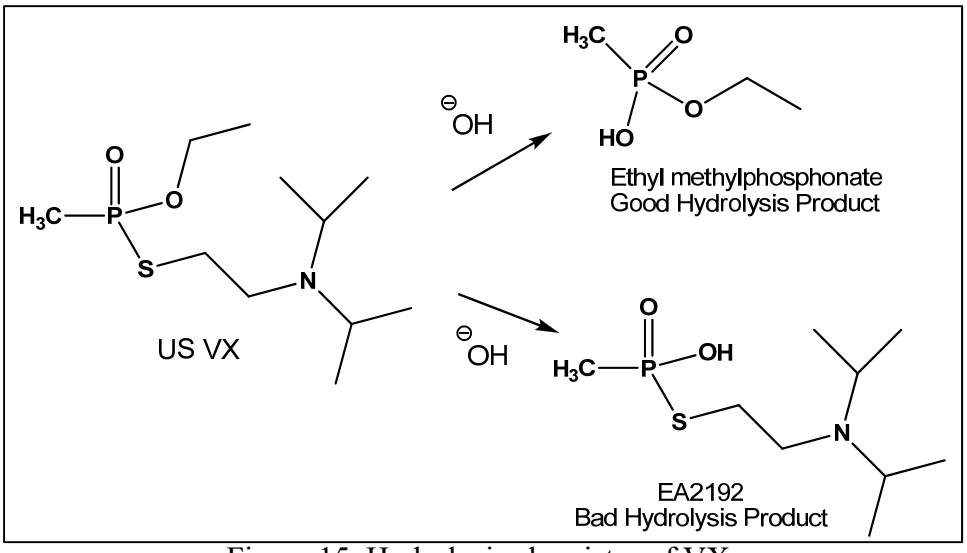

Figure 15. Hydrolysis chemistry of VX.

At room temperature, EA 2192 is a white solid. It is extremely soluble and stable in water at neutral and alkaline pHs. It proved to be more stable during hydrolysis than VX (i.e., in a solution of 0.1 N NaOH at 25 °C, no significant hydrolysis occurred within 12 days). The carbon partition coefficient (log K_{OC}) of EA 2192 is 1.90, which indicates a low potential to

adsorb onto soil. However, the octanol/water partition coefficient (log K_{OW}) is 0.96, which indicates small bioconcentration factors for aquatic life.

We have prepared a series of model compounds[47,48] for EA 2192 that are based on methyl phosphonic acid containing a variety of leaving groups (**7a–e**). Preliminary kinetics studies were performed of the decomposition of EA 2192 model compounds using lanthanum triflate solutions in the range of 1×10^{-4} to 2.5×10^{-3} M. The pH was controlled using various noninhibitory buffers, including *N*-methylimidazole ($^{s}_{s}$pH of 7.60), *N*-ethylmorpholine ($^{s}_{s}$pH of 8.28), and triethylamine ($^{s}_{s}$pH of 10.78), which were partially neutralized with triflic acid. Reaction progress was monitored using UV-vis spectroscopy.

Plots of k_{obs} as opposed to $[La^{3+}]_t$ data for methanolysis of **7a** are somewhat unusual, particularly at low pH values. At $^{s}_{s}$pH of 8.4–8.7, the catalytic effect of $[La^{3+}]_t$ changes rapidly to attenuation of the catalysis with further increase in the La^{3+} concentration. In the example presented in Figure 16 ($^{s}_{s}$pH of 8.4), k_{obs} decreased from 5×10^{-4} M < $[La^{3+}]$ < 1.5×10^{-3} and then remained almost constant with increasing $[La^{3+}]_t$. In the case of high $^{s}_{s}$pH values (Figure 17; $^{s}_{s}$pH of 11.7), the rate constant increased with $[La^{3+}]_t$, and then saturation phenomena were observed.

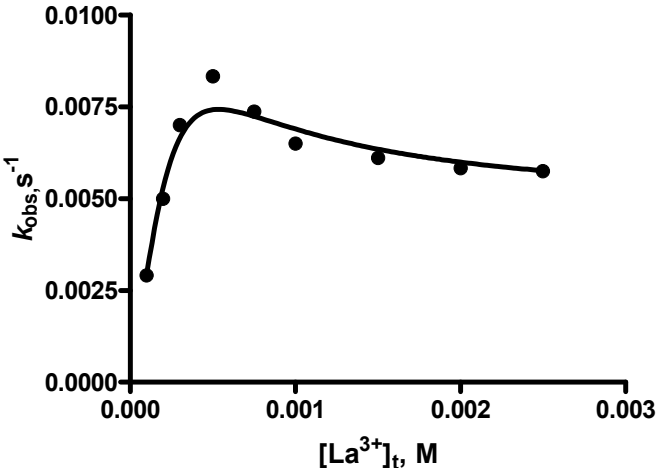

Figure 16. Plot of pseudo-first-order rate constant for the methanolysis of **7a** (1×10^{-4} M) vs $La(OTf)_3$ at 25.0 ± 0.1 °C and a $^{s}_{s}$pH of 8.4 in 0.04 M *N*-ethylmorpholine buffer.

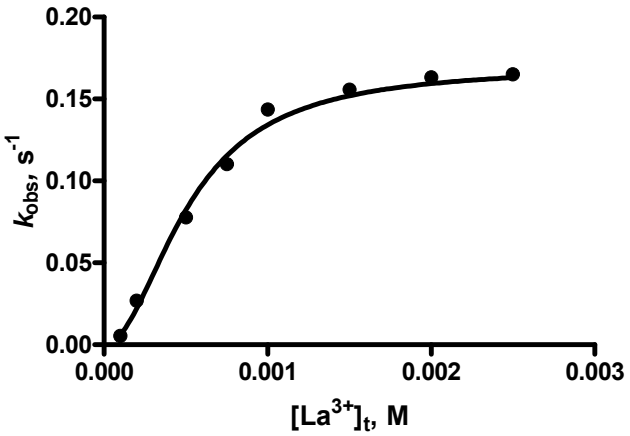

Figure 17. Plot of pseudo-first-order rate constant for the methanolysis of **7a** (1×10^{-4} M) vs $La(OTf)_3$ at 25.0 ± 0.1 °C and a ${}^{s}_{s}pH$ of 11.7 in 0.04 M triethylamine buffer.

Experimental data from the plots of k_{obs} as opposed to $[La^{3+}]_t$ data for methanolysis of **7** were analyzed in terms of the second-order rate constant for the reaction of **7** with $La^{3+}(CH_3O^-)_m$ (k_1) and pseudo first-order-rate constant for methanolysis of complex $(La^{3+})_2$:**1**:$(CH_3O^-)_n$ (k_{cat}). Representative data for compound **7b** at various ${}^{s}_{s}pH$ values are provided in Table 4.

Table 4. ${}^{s}_{s}pH$ Dependence of the Second-Order Rate Constant for the Reaction of **7b** with $La^{3+}(CH_3O^-)_m$(k_1) and Pseudo First-Order-Rate Constant for Methanolysis of $(La^{3+})_2$:**1**:$(CH_3O^-)_n$ (k_{cat}) at 25.0 ± 0.1 °C

${}^{s}_{s}pH$	k_1 (M^{-1} s^{-1})	10^3 k_{cat} (s^{-1})
7.6	3.40 ± 0.30	0.32
8.4	5.96 ± 0.60	0.58
8.9	8.75 ± 0.62	3.33
9.9	15.0 ± 1.2	7.33
10.9	10.8 ± 1.0	12.16
11.7	5.85 ± 0.40	18.33

7.2 Effect of Leaving Group on Reactivity of Model Compounds and Prediction of EA 2192 Reactivity

Figure 17 shows the Brønsted plots of log k_{cat} as opposed to experimentally determined ${}^{s}_{s}pK_a^{HSAr}$ values for the corresponding thiophenols for the La^{3+}-promoted cleavage of **7a–e** at ${}^{s}_{s}pH$ 8.4 and 11.7. In both cases, the plots are straight lines described by eqs 2 and 3.

$$\log k_{cat}^{8.4} = (4.02 \pm 0.36) - (0.69 \pm 0.03)\,{}^{s}_{s}pK_a^{HSAr} \qquad r^2 = 0.99 \qquad (2)$$

$$\log k_{cat}^{11.7} = (3.79 \pm 0.35) - (0.52 \pm 0.03)\,{}^{s}_{s}pK_a^{HSAr} \qquad r^2 = 0.99 \qquad (3)$$

From our previous report of La^{3+}-promoted methanolysis of VX analogues, the predicted value of ${}^{s}_{s}pK_a$ for $HSCH_2CH_2N(CH(CH_3)_2)_2$ was ~9.54. Therefore, the predicted k_{cat} values computed from eqs 2 and 3 for EA 2192 were 2.74×10^{-3} and 6.75×10^{-2} s^{-1} at ${}^{s}_{s}pH$ values of 8.4 and 11.9, respectively.

To provide a better forecast of the EA 2192 decomposition rate using the MICA solution, we have studied the decomposition rates of the **7a–e** series of model compounds in MICA solution. The data presented in Figure 18 and the Brønsted correlation in eq 4 indicate that the rate of decomposition of model compounds in MICA solution is closely correlated with the pseudo-first-order rate constant for methanolysis of $(La^{3+})_2$:Sub:$(CH_3O^-)_n$ (k_{cat}).

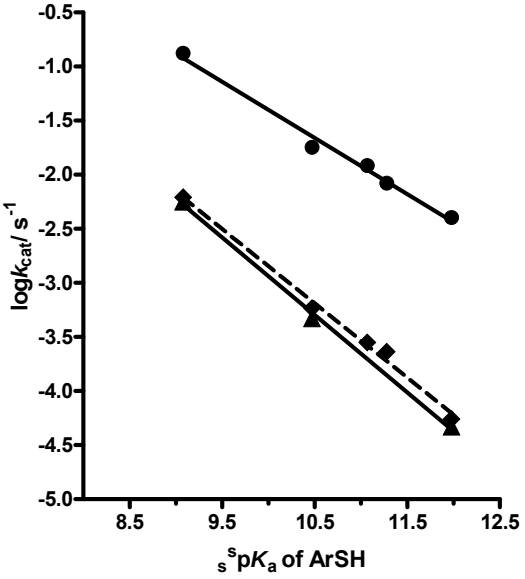

Figure 18. Brønsted plots for the La^{3+}-catalyzed methanolysis of EA 2192 analogues **7** (solid line) determined at ${}^{s}_{s}pH$ of 11.7 and 25.0 ± 0.1 °C temperature (where $\log k_{cat}^{8.4} = (4.02 \pm 0.36) - (0.69 \pm 0.03)\,{}^{s}_{s}pK_a^{HSAr}$ and $r^2 = 0.99$) and (dashed line) determined at ${}^{s}_{s}pH$ of 8.4 and 25.0 ± 0.1 °C temperature (where $\log k_{cat}^{8.4} = (3.79 \pm 0.35) - (0.52 \pm 0.03)\,{}^{s}_{s}pK_a^{HSAr}$ and $r^2 = 0.99$). Solid ▲ line indicates log k_{cat} vs ${}^{s}_{s}pK_a^{HSAr}$ for the reactions between **7a–e** and MICA (i.e., $\log k_{cat}^{MICA} = (4.22 \pm 0.33) - (0.72 \pm 0.03)\,{}^{s}_{s}pK_a^{HSAr}$ and $r^2 = 0.99$).

$$\log k_{cat}^{MICA} = (4.22 \pm 0.33) - (0.72 \pm 0.03)\,{}^{s}_{s}pK_a^{HSAr} \quad r^2 = 0.99 \qquad (4)$$

7.3 Results for Ethanolamine/La^{3+}-Mediated Decomposition of Phosphonate Substrates

Tables 5–7 show the concentration dependence of various La-based catalysts in ethanolamine, ethanolamine/ethanol mixture, and ethanolamine/methanol mixture, and Tables 8–16 show the effects of mixing various solutions.

Table 5. Concentration Dependence of La-Based Catalysts in Ethanolamine toward Solvolysis of *p*-Nitrophenyl Ethyl Methylphosphonate (0.02 mM) at 25 °C

[La]/k_{obs} (min^{-1}) (mM)	$La(OTF)_3$	$La(Ms)_3$
1	2.69	2.96
2	4.44	4.55
3	6.93	7.10
5	10.30	11.65

Table 6. Concentration Dependence of La-Based Catalysts in Ethanolamine/Ethanol Mixture (70:30% v/v) toward Solvolysis of *p*-Nitrophenyl Ethyl Methylphosphonate (0.02 mM) at 25 °C

[La]/k_{obs} (min^{-1}) (mM)	$La(OTF)_3$	$La(Ms)_3$
1	2.69	2.34
2	4.41	3.86
3	8.18	6.41
5	12.35	11.07

Table 7. Concentration Dependence of La-Based Catalysts in Ethanolamine/Methanol Mixture (70:30% v/v) toward Solvolysis of *p*-Nitrophenyl Ethyl Methylphosphonate (0.02 mM) at 25 °C

[La]/k_{obs} (min^{-1}) (mM)	$La(OTF)_3$	$La(Ms)_3$
1	2.03	2.83
2	3.46	4.82
3	9.48	7.05
5	22.51	15.53

Table 8. Effect of Extraneous Water Added to the 5 mM Solution of $La(OTf)_3$ in Ethanolamine and Ethanolamine/Ethanol (70:30% v/v) and Ethanolamine/Methanol (70:30% v/v) Mixtures on the Solvolysis Rate of *p*-Nitrophenyl Ethyl Methylphosphonate (0.02 mM) at 25 °C

$\%H_2O/k_{obs}$ (min^{-1}) (%)	Ethanolamine + 30% Ethanol	Ethanolamine + 30% Methanol	Ethanolamine
0	12.35	22.51	10.30
1	6.08	8.32	5.53
2	3.87	5.20	4.26
5	2.60	2.68	3.91
10	1.07	1.88	1.86
20	0.57	1.06	1.47

Table 9. Effects of Fluoride Anion Addition to the 5 mM $La(OTf)_3$ Solution in Ethanolamine and Ethanolamine/Ethanol Mixture (70:30% v/v) and Ethanolamine/Methanol (70:30% v/v) Mixtures on the Solvolysis Rate of *p*-Nitrophenyl Ethyl Methylphosphonate (0.02 mM) at 25 °C

$[F^-]/k_{obs}$ (min^{-1}) (mM)	Ethanolamine + 30% Ethanol	Ethanolamine + 30% Methanol	Ethanolamine
0	12.35	22.51	10.30
5	7.51	8.05	5.84
10	3.43	2.89	1.91
20	0.79	0.78	1.14

Table 10. Effects of Extraneous Water Added to the 5 mM $Sm(OTf)_3$ Solution in Ethanolamine and Ethanolamine/Ethanol Mixture (70:30% v/v) on the Solvolysis Rate of *p*-Nitrophenyl Ethyl Methylphosphonate (0.02 mM) at 25 °C

$\%H_2O/k_{obs}$ (min^{-1}) (%)	Ethanolamine + 30% Methanol	Ethanolamine
0	13.67	6.58
1	11.56	6.42
2	12.75	5.62
5	3.96	5.37
10	1.93	2.79

Table 11. Effects of $La(OTf)_3$ Aging in the Presence of 20% (v/v) Water on the Rate Constant for Reaction with *p*-Nitrophenyl Ethyl Methylphosphonate in Ethanolamine and Ethanolamine/Ethanol Mixture (70:30% v/v) at 25 °C

Time of Aging (min)/k_{obs}(min^{-1})	Ethanolamine	70% Ethanolamine + 30% Ethanol
0	1.41	0.70
30	1.29	0.52
60	1.01	0.41
120	0.94	0.50
180	0.91	0.36
1440	0.87	0.24

Table 12. Effects of $Sm(OTf)_3$ Aging in the Presence of 20% (v/v) Water on the Rate Constant for the Reaction with *p*-Nitrophenyl Ethyl Methylphosphonate in Ethanolamine and Ethanolamine/Ethanol Mixture (70:30% v/v) at 25 °C

Time of Aging (min)/k_{obs}(min^{-1})	Ethanolamine	70% Ethanolamine + 30% Ethanol
0	1.18	0.52
30	0.81	0.43
60	0.84	0.31
120	0.80	0.37
180	0.82	0.30
1440	0.74	0.33

Table 13. Effects of Extraneous Water Added to the 100 mM $La(OTf)_3$ Solution in Ethanolamine and Ethanolamine/Ethanol Mixture (70:30% v/v) on the Paraoxon (0.02 mM) Solvolysis Rate at 25 °C

H_2O%/k_{obs} (min^{-1})	Ethanolamine	Ethanolamine + 30% Ethanol
0	34.67	25.30
1	13.59	5.23
2.5	4.01	1.50
5	1.16	0.87
10	0.64	0.24
15	0.38	—

—: data not available.

Table 14. Effects of Extraneous Water Added to the 50 mM $La(OTf)_3$ Solution in Ethanolamine and Ethanolamine/Ethanol Mixture (70:30% v/v) on the Paraoxon (0.02 mM) Solvolysis Rate at 25 °C

H_2O%/k_{obs} (min^{-1})	Ethanolamine	Ethanolamine + 30% Ethanol
0	24.91	14.21
1	4.87	2.92
2.5	1.29	0.40
5	0.38	0.42
10	0.27	0.13
15	0.24	—
20	0.15	—
30	0.15	—

—: data not available.

Table 15. Effects of Extraneous Water Added to the 30 mM $La(OTf)_3$ Solution in Ethanolamine and Ethanolamine/Ethanol Mixture (70:30% v/v) on the Paraoxon (0.02 mM) Solvolysis Rate at 25 °C

H_2O%/k_{obs} (min^{-1})	Ethanolamine	Ethanolamine + 30% Ethanol
0	12.8	13.0
1	2.8	1.3
2.5	0.51	0.21
5	0.19	0.14
10	0.15	0.13

Table 16. Effects of Extraneous Water Added to the 50 mM $Sm(OTf)_3$ Solution in Ethanolamine and Ethanolamine/Ethanol Mixture (70:30% v/v) on the Paraoxon (0.02 mM) Solvolysis Rate at 25 °C

H_2O%/k_{obs} (min^{-1})	Ethanolamine	Ethanolamine+ 30% Ethanol
0	6.85	3.73
1	4.09	1.61
2.5	2.44	0.98
5	1.45	0.73
10	0.57	0.28

7.4 Destruction of CWAs Using Force-to-Fail Criteria

Based on the experimental procedures described in Section 6.5, several catalytic systems in methanol, ethanol, and ethanolamine, containing La^{3+}, Sm^{3+}, buffer, and other ingredients, were formulated and tested at ECBC. These were evaluated for their efficacy in

decomposing OP CWAs, namely tabun (GA); GB; GD; GF; VX; RVX; and phosphorodithioic acid, methyl-*S*,*S*-bis[diethylamino]ethyl ester (RV-bis; CAS no. 92030-06-3; a component of munitions-grade RVX) that is reported to be as toxic as RVX. The results are summarized in Table 17.

Table 17. Catalytic Systems Formulated and Tested for Efficacy in Decomposing OP CWAs

Agent[a]	Decontamination System	Load at Force to Fail (%)
GA (tabun)	S4 (La^{3+}/methanol)	>29.50
GB (sarin)	S4 (La^{3+}/methanol)	2.50
GD (soman)	S4 (La^{3+}/methanol)	2.50
GF (cyclosarin)	S4 (La^{3+}/methanol)	2.50
GF (cyclosarin)	S5 (Sm^{3+}/methanol)	6.00
GF (cyclosarin)	E4 (La^{3+}/ethanol)	3.90
GF (cyclosarin)	E5 (Sm^{3+}/ethanol)	6.70
USVX (CASARM)	S4 (La^{3+}/methanol)	24.90
USVX (munitions)	S4 (La^{3+}/methanol)	~15
RVX (CASARM)	S4 (La^{3+}/methanol)	20.00
USVX (CASARM)	S4a (La^{3+}/methanol)	34.00
USVX (munitions)	S4a (La^{3+}/methanol)	33.70
USVX (CASARM)	E4 (La^{3+}/methanol)	19.20
RVX (CASARM)	E4 (La^{3+}/methanol)	23.90
GF (cyclosarin)[b]	S12 (La^{3+}/MEA)	>8.00
USVX (CASARM)	S12 (La^{3+}/MEA)	17.20
USVX (CASARM)	S14 (Sm^{3+}/MEA)	5.36
RV-bis[c]	S4 (La^{3+}/methanol)	21.20

[a] All agents are chemical agent standard analytical reference materials (CASARMs) with at least 95% purity.
[b] G agents, such as GF, react exothermically with MEA. Because of the heat produced, the force-to-fail experiment in this case did not proceed beyond the 8.00% indicated.
[c] Toxic impurity produced during synthesis of RVX.

7.5 TNO-Agent Results

Independent, contract laboratory testing at the Netherlands Organisation for Applied Scientific Research (TNO; Rijswijk, the Netherlands) was performed on the solution S4 (La^{3+}/methanol). The activities for GA, GD, USVX, and sulfur mustard (HD) were studied at a 50:1 (v/v) challenge (50 parts of System 4 decontaminant solution and 1 part CWA). Analyses were performed and reaction products were obtained by NMR or gas chromatography–mass spectrometry (GC-MS), and in the case of VX, by liquid chromatography–mass spectrometry (LC-MS). Given the predicted high efficiency of the decontamination method, all the samples were analyzed as quickly as possible after the addition of all the components. This involved quenching the reaction by adding HCl to the decontaminating solution that contained the agent, before performing NMR analysis. MICA was also tested on solid surfaces, namely panels coated with chemical agent-resistant coating (CARC). The panels were coated with 10 g/m^2 CWA, and

after a 10 min decontamination time, the reactions were stopped, and residual agent was solvent-extracted and analyzed using GC-MS.

In the 50:1 challenge liquid-solution tests, all of the OP agents (GA, GD, and VX) were destroyed in less than 30s (the minimal possible testing time), and no residual nerve agents were detected in solution by GC-MS at a detection limit of <200 ng/mL. After completion of each reaction, only the nontoxic corresponding *O*-methylation product was identified for each nerve agent. Notably, it was shown that the possible toxic degradation product of VX, EA 2192 (an often-found product of decontamination in aqueous solution), was not formed during the decomposition of USVX (at a detection limit of <1 ppm).

The solution also decontaminated nerve agents on CARC panels (at a loading of 10 g/m^2) within 10 min of using a minimal amount of the solution (<1 mL/cm^2) with no scrubbing or agitation. The efficiency of the decontamination was >99%, and in most cases, >99.9% (Table 18). In the case of HD, although the solution removed 95% of the material from the CARC panel within 10 min, the blister agent was not destroyed but simply removed through its solubility in methanol. This suggests that System 4 might have practical use for HD removal from surfaces; however, the recovered solution would still contain active material that requires post-treatment.

Table. 18. Decontamination Efficiency of Decontamination System against GA, GD, VX, and HD on CARC Panels

Agent (10 g/m^2)	Reaction Time	Decontamination Efficiency (%)[a]
GA	10 min	>99.9
GD		99.2
VX		>99.9
HD		95

[a]Detection limit = 0.5 µg/cm^3. Amount corrected for extraction efficiencies.

7.6 Agent Testing at Research Institute of Hygiene, Occupational Pathology, and Human Ecology (RIHOPHE; St. Petersburg, Russia)

Further testing of MICA was performed in the spring of 2009 in collaboration with Queen's University (Ontario, Canada) and RIHOPHE. The testing involved a 50:1 challenge of RVX (20 mg/mL or 20,000 ppm), and analysis of the reaction mixture was performed using direct-injection GC-MS techniques. These tests established that after 1 min, no residual RVX was present in the solution (at a detection limit of <1 ppm), which indicated that >99.995% decontamination had occurred within that time.

8. DISCUSSION

8.1 Destruction Efficiency of MICA

A summary of the force-to-fail agent results described in the preceding sections clearly show that System 4 (La^{3+}/methanol) was extremely efficient at the transesterification decomposition of nonfluoride agents (i.e., GA and V-class agents); agent loads of 15–35% were generated using the designated reaction criteria. Because of the interaction and inhibition of fluoride with the La^{3+} metal ion, the G-class agents were decomposed at higher efficiencies than those at the 1:50 ratio, but those results were not nearly as impressive as the results for nonfluoride-releasing agents. Lanthanide ions are highly Lewis acidic; therefore, their interactions with fluoride anions are very strong and inhibitory. This inhibition effect was ameliorated by Sm^{3+}substitution as the metallic ion catalysis progressed (at loads of ~6–7%). Attempts to use other strategies to address this fluoride ion issue have yet to yield effective solutions for obtaining loads comparable with those obtained for GA and V-class agents.

8.2 Alternative Solvents

MICA is a lanthanide/methanol-based decontamination solution that exhibits extremely high activity for the decomposition of OP CWAs (such as G- and V-class agents). However, many issues with MICA must be addressed. One is the perceived toxicity and flammability of the methanol-based solution. A possible method for resolving this problem is to use ethanol as the main component in the decontamination system. Ethanol is generally considered to be far less toxic than other alcohols, and it has a higher flash point than methanol, which should, to a certain degree, mitigate flammability issues. As indicated by the summary of agent results (Table 17), substitution of ethanol for methanol (as in Systems E4 and E5) does not significantly affect the destruction efficiency. For example, comparison of the two ethanol-based formulations of Systems E4 and E5 with the methanol formulation of System S4 at the 5% load factor with RVX showed that within the first time point during the NMR experiment (~3.5 min), all three provided baseline VX destruction (the peak at ~58 ppm destroyed and ester peaks at 31–33 ppm were phosphorus peaks). Force-to-fail experiments were above the 5% load. Both VX and RVX yielded loads comparable to those observed in the System 4 experiments. Continued experimentation with ethanolamine clearly indicated that this solvent can be substituted for methanol and ethanol. Recent work also indicated that mixtures of all three alcohols were effective as supporting solvents for this chemistry. Thus, the flash point of the solvent can be adjusted over a large range and “tuned” to the application.

8.3 Effects of Water on Reactivity

A few examples of full-strength decontamination solutions were created, and in all cases, they had very high reactivities for the decomposition of the chemical weapons model compound, paraoxon. The ability to withstand the inhibitory effects of extraneous moisture was tested, and it was demonstrated that a samarium-based catalytic system had the best resistance to extraneous moisture. This is important for any “real-life” scenario. These results will allow us to formulate a metal ion-based catalytic system for the decomposition of live OP CWAs that is suitable for any given application and then proceed to testing with live agents.

8.4 Simulant Reactivity

Two nonagent simulants for V-agents (*O*-ethyl-*S*-ethyl methylphosphonate and *O*-ethyl-*S*-ethyl phenylphosphonate) were tested at the 5% load with the decontamination systems described in Table 17. All were degraded in a very similar manner to V-agents, although at a somewhat slower rate. This observation provides nonclassified laboratories with an acceptable simulant for V-agents, so that data related to the mechanism of transesterification can be obtained before the expense of agent testing is incurred. Testing of the G-agent simulant directly against GF is scheduled for future work.

8.5 Production and Decomposition of EA 2192

There is no evidence that EA 2192 was produced in any of the solvent combinations reported herein. Preliminary results indicated that Systems S4 (La^{3+}/methanol) and S12 (La^{3+}/MEA) appeared to slowly decompose EA 2192. Exact kinetics results have not yet been obtained, and future work will address this result.

8.6 Low-Level Residual Agent Concentration

In the force-to-fail experimental design, the use of ^{31}P NMR limited the detection limit of residual agents to approximately 0.1–0.05%. The exact residual agent concentration was not part of the original ECBC analytical protocol. Results from TNO and RIHOPHE (obtained using GC-MS and LC-MS techniques) indicated considerably greater destruction efficiency. Thus, at the end of the project period of performance, the adaption of two new techniques was in progress: a liquid chromatography–tandem mass spectroscopy technique based on the work of Evans et al.[49] and an enzyme-inhibition assay.[50] Future evaluation of this chemistry will include an attempt to use these procedures to better understand low-level residual agent concentrations.

9. CONCLUSIONS

Metal ion-catalyzed methanolysis provides a simple yet effective methodology for the decontamination of neutral OPs of the phosphate, phosphonate, phosphorothioate, and phosphonothioate classes. The most effective catalysts to date for alcoholysis of the compounds containing the P=O unit are those containing lanthanide ions, particularly La^{3+}, and certain complexes of transition metal ions, notably Zn^{2+} and Cu^{2+}, at near-neutral ${}^{s}_{s}pH$ values. MICA, containing La^{3+} buffered at a ${}^{s}_{s}pH$ of nine, was shown to catalyze the decontamination of OP chemical weapons, including GA, GB, GD, and other G-agents as well as USVX and RVX. Nontoxic products using methanolysis were developed. On the other hand, La^{3+}-based catalysts were ineffective for the decomposition of neutral OP materials that contain P=S, some of which can be used as pesticides.

LITERATURE CITED

1. United States Chemical Weapons Convention Website Home Page. http://www.cwc.gov/cwc_treaty.html (accessed 4 June 2013).

2. Morales-Rojas, H.; Moss, R.A. Phosphorolytic Reactivity of *o*-Iodosylcarboxylates and Related Nucleophiles. *Chem. Rev.* **2002,** *102,* 2497–2521.

3. Pearson, G.S.; Magee, R.S. Critical Evaluation of Proven Chemical Weapon Destruction Technologies (IUPAC Technical Report). *Pure Appl. Chem.* **2002,** *74,* 187–316.

4. Yang, Y.C.; Baker, J.A.; Ward, J.R. Decontamination of Chemical Warfare Agents. *Chem. Rev.* **1992,** *92,* 1729–1743.

5. Yang, Y.C. Chemical Detoxification of Nerve Agent VX. *Acc. Chem. Res.* **1999,** *32,* 109–115.

6. Yang, Y.C. Chemical Reactions for Neutralizing Chemical Warfare Agents. *Chem. Ind. (London, U.K.)* **1995,** *9,* 334–337.

7. Brown, R.S.; Neverov, A.A. Acyl and Phosphoryl Transfer to Methanol Promoted by Metal Ions. *J. Chem. Soc. Perkin Trans.* **2002,** *2,* 1039.

8. Brown, R.S.; Neverov, A.A.; Tsang, J.S.W.; Gibson, G.T.T.; Montoya-Pelaez, P.J. Bader Award Lecture Metal-Ion-Catalyzed Acyl and Phosphoryl Transfer Reactions to Alcohols: La^{3+}-Promoted Alcoholysis of Activated Amides, Carboxylate Esters, and Neutral Organophosphorus Esters. *Can. J. Chem.* **2004,** *82,* 1791–1805.

9. Brown, R.S.; Neverov, A.A. *Advances in Physical Organic Chemistry*; Richard, J.P., Ed.; Vol. 42; Elsevier: San Diego, CA, 2007, p 271.

10. Yang, H.; Carr, P.D.; McLoughlin, S.; Yu, L.J.W.; Horne, I.; Qiu, X.; Jeffries, C.M.J.; Russell, R.J.; Oakeshott, J.G.; Ollis, D.L. Evolution of an Organophosphate-Degrading Enzyme: A Comparison of Natural and Directed Evolution. *Protein Eng.* **2003,** *16,* 135–145.

11. Jackson, C.J.; Foo, J.-L.; Kim, H.-K.; Carr, P.D.; Liu, J.-W.; Salem, G.; Ollis, D.L. In Crystallo Capture of a Michaelis Complex and Product-Binding Modes of a Bacterial Phosphotriesterase. *J. Mol. Biol.* **2008,** *375,* 1189–1196.

12. Kim, J.; Tsai, P.-C.; Chen, S.-L.; Himo, F.; Almo, S.C.; Raushel, F.M. Structure of Diethyl Phosphate Bound to the Binuclear Metal Center of Phosphotriesterase. *Biochemistry* **2008,** *47,* 9497–9504.

13. Lipscomb, W.N.; Straeter, N. Recent Advances in Zinc Enzymology. *Chem. Rev.* **1996,** *96,* 2375–2434.

14. Coleman, J.E. Zinc Enzymes. C*urr. Opin. Chem. Biol.* **1998,** *2*, 222–234.

15. Cowan, J.A. Metal Activation of Enzymes in Nucleic Acid Biochemistry. *Chem. Rev.* **1998,** *98,* 1067–1088.

16. Davies, J.F.; Hostomska, Z.; Hostomsky, Z; Jordan, S.R.; Matthews, D.A. Crystal Structure of the Ribonuclease H Domain of HIV-1 Reverse Transcriptase. *Science* **1991,** *252,* 8–95.

17. Beese, L.S.; Steitz, T.A. Structural Basis for the 3'-5' Exonuclease Activity of *Escherichia coli* DNA Polymerase I: A Two Metal Ion Mechanism. *EMBO J.* **1991,** *10,* 25–33.

18. Lahm, A.; Volbeda, A.; Suck, D. Crystallisation and Preliminary Crystallographic Analysis of P1 Nuclease from Penicillium Citrinum. *J. Mol. Biol.* **1990,** *215,* 207–210.

19. Gani, D.; Wilkie, J. Stereochemical, Mechanistic, and Structural Features of Enzyme-Catalyzed Phosphate Monoester Hydrolysis. *Chem. Soc. Rev.* **1995,** *24,* 55–63.

20. Omburo, G.A.; Kuo, J.M.; Mullins, L.S.; Raushel, F.M. Characterization of the Zinc Binding Site of Bacterial Phosphotriesterase. *J. Biol. Chem.* **1992,** *267,* 13278–13283.

21. Cleland, W.W.; Frey, P.A.; Gerlt, J.A. The Low Barrier Hydrogen Bond in Enzymic Catalysis. *Biol. Chem*. **1998,** *273,* 25529–25532.

22. Tsang, J.S.; Neverov, A.A.; Brown, R.S. Billion-Fold Acceleration of the Methanolysis of Paraoxon Promoted by $La(OTf)_3$ in Methanol. *J. Am. Chem. Soc.* **2003,** *125,* 7602–7607.

23. Gibson, G.; Neverov, A.A.; Brown, R.S. Potentiometric Tritration of Metal Ions in Methanol. *Can. J. Chem.* **2003,** *81,* 495–504.

24. Lewis, R.E.; Neverov, A.A.; Stan Brown, R.S. Mechanistic Studies of La^{3+} and Zn^{2+}-catalyzed Methanolysis of *O*-ethyl *O*-aryl Methylphosphonate Esters. An Effective Solvolytic Method for the Catalytic Destruction of Phosphonate CW Simulants. *Org. Biomol. Chem.* **2005,** *3,* 4082–4088.

25. Desloges, W.; Neverov, A.A.; Brown, R.S. Zn^{2+}-Catalyzed Methanolysis of Phosphate Triesters: A Process for Catalytic Degradation of the Organophosphorus Pesticides Paraoxon and Fenitrothion. *Inorg. Chem.* **2004,** *43,* 6752–6761.

26. Melnychuk, S.A.; Neverov, A.A.; Brown, R.S. Catalytic Decomposition of Simulants for Chemical Warfare V Agents: Highly Efficient Catalysis of the Methanolysis of Phosphonothioate Esters. *Angew. Chem. Int. Ed. Engl.* **2006,** *45,* 1767–1770.

27. Neverov, A.A.; Brown, R.S. Cu(II)-Mediated Decomposition of Phosphorothioate P=S Pesticides. Billion-Fold Acceleration of the Methanolysis of Fenitrothion Promoted by a Simple Cu(II)-Ligand System. *Org. Biomol. Chem*. **2004,** *2,* 2245–2248.

28. Beaudry, W.T.; Szafraniec. L.L.; Leslie, R.D. *Reactions of Chemical Warfare Agents with DS-2: Product Identification by NMR. 1. Organophosphorus Compounds*; CRDEC-TR-364; U.S. Army Edgewood Research, Development, and Engineering Center: Aberdeen Proving Ground, MD, 1992; UNCLASSIFIED Report (ADA254284).

29. Sheluchenko, V.V.; Durst, H.D. *Russian-American Experiments; Annotated Report, Two-Stage Process of Sarin, Soman, and Destruction*; BNI Job No. 22911; Bechtel National, Inc.: McLean, VA, 1995.

30. Morrissey, K.M.; Brickhouse, M.D.; Raghuveer, K.; Williams, B.R.; and Heykamp, L.S. *Chemical Characterization of Reaction Masses, Bitumenized Reaction Masses, and Distillates Produced During the Russian-American Joint Evaluation Program (RAJEP), Final Comprehensive Report*; EAI Report 56/96/001F; EAI Corporation: Abingdon, MD, 1996.

31. Brickhouse, M.D.; Rees, M.; O'Connor, R.J.; Durst, H.D. *Nuclear Magnetic Resonance (NMR) Analysis of Chemical Agents and Reaction Masses Produced by Their Chemical Neutralization*; ERDEC-TR-449; U.S. Army Edgewood Research, Development and Engineering Center: Aberdeen Proving Ground, MD, 1997; UNCLASSIFIED Report (ADA339308).

32. McGarvey, D.J; Durst, H.D; Creasy, W.R.; Ruth, J.L.; Morrissey, K.M.; Stuff, J.R. *Chemical Analysis and Reaction Kinetics of EA-2192 in Decontamination Solution for the MMD-1 Project*; ECBC-TR-282; U.S. Army Soldier and Biological Chemical Command: Aberdeen Proving Ground, MD, 2003; UNCLASSIFIED Report (ADA416809).

33. Morrissey, K.M.; Williams, B.R.; Cheicante, R.; Stuff, J.R.; Durst, H.D. *Quantitative and Qualitative Gas Chromatographic Analysis of Reaction Masses Produced from Chemical Neutralization of GB with Monoethanolamine*; ECBC-TR-041; U.S. Army Soldier and Biological Chemical Command: Aberdeen Proving Ground, MD, 1999; UNCLASSIFIED Report (ADA368372).

34. Morrissey, K.M.; Williams, B.R.; Ruth, J.L.; Stuff, J.R.; Durst, H.D. *Quantitative and Qualitative Gas Chromatographic Analysis of Reaction Masses Produced from Chemical Neutralization of VX with Monoethanolamine*; ECBC-TR-042; U.S. Army Soldier and Biological Chemical Command: Aberdeen Proving Ground, MD, 1999; UNCLASSIFIED Report (ADA368373).

35. *Evaluation of the Chemistry which Supports VX Neutralization in the Munitions Management Device-1 (MMD-1)*; Durst, H.D., Ed.; The U.S. Army Chemical Material Agency's Non-Stockpile Chemical Materiel Project: Aberdeen Proving Ground, Edgewood Area, MD, 1997; UNCLASSIFIED Report.

36. *Evaluation of the Chemistry which Supports GB Neutralization in the Munitions Management Device-1 (MMD-1)*; Durst, H.D., Ed.; The U.S. Army Chemical Material Agency's Non-Stockpile Chemical Materiel Project: Aberdeen Proving Ground, MD, 1997; UNCLASSIFIED Report.

37. DeBruin, K.E.; Tang, C.I.W.; Johnson, D.M.; Wilde, R.L. Kinetic Facial Selectivity in Nucleophilic Displacements at Tetracoordinate Phosphorus: Kinetics and Stereohemistry in the Reaction of Sodium Ethoxide with O,S-Dimethyl Phenylphosphonothioate. *J. Am. Chem. Soc.* **1989,** *111,* 5871–5879.

38. Hollingshaus, J.G.; Armstrong, D.; Tois, R.F.; McCloud, L.; Fukuto, T.R. Delayed Toxicity and Delayed Neurotoxicity of Phosphonothioate and Phosphonothioate Esters. *J. Toxicol. Environ. Health*, **1981,** *8,* 619–627.

39. Hollingshaus, J.G.; Nishioka, T.; March, R.B.; Fukuto, T.R. Effect of Impurities on the Delayed Neurotoxicity of *O*-(4-bromo-2,5-dichlorophenyl) *O*-Ethyl Phenylphosphonothioate Administered Orally to Hens. *J. Agric. Food Chem.* **1981,** *29,* 593–600.

40. Spector, W.S. *Handbook of Toxicology*; W.B. Saunders Company: St. Louis, MO, 1956; Vol. 1, p 4.

41. Wiles, J.S.; Manthei, J.H.; Christesen, M.K. *Toxicological Evaluation in Animals of Simulant Components, Mixtures, and/or Reaction Products for Use in Testing the XM736 8-Inch Binary VX Projectiles*; ARCSL-TR-79051; U.S. Army Armament Research and Development Command: Aberdeen Proving Ground, MD, 1980; UNCLASSIFIED Report (ADB050332).

42. Kuo, L.Y.; Adint, T.T.; Akagi, A.E.; Zakharov, L. Degradation of a VX Analogue: First Organometallic Reagent to Promote Phosphonothioate Hydrolysis through Selective P–S Bond Scission. *Organometallics* **2008,** *27* (11), 2560–2564.

43. Seabolt, E.E.; Ford, W.T. Alkaline Hydrolysis of *O*,*S*-Diethyl Phenylphosphonothioate and *p*-Nitrophenyl Diethyl Phosphate in Latex Dispersions. *Langmuir* **2003,** *19* (13), 5378–5382.

44. Wagner, G.W.; Bartram, P.W. Reactions of VX, HD, and Their Simulants with NaY and AgY Zeolites. *Langmuir* **1999,** *15* (23), 8113–8118.

45. Moss, R.A.; Morales-Rojas, H.; Zhang, H.; Park, B.-D. Cleavage of VX Simulants by Micellar Iodoso- and Iodoxybenzoate. *Langmuir* **1999,** *15* (23), 8113–8118.

46. Berg, F.J.; Moss, R.A.; Yang, Y.-C.; Zhang, H. Cleavage of Phenylphosphonothioates by Hydroxide Ion and by Micellar Iodosobenzoate. *Langmuir* **1995,** *11* (2), 411–413.

47. Dhar, B.B.; Edwards, D.R.; Brown, R.S. A Study of the Kinetics of La^{3+}-Promoted Methanolysis of *S*-Aryl Methylphosphonothioates: Possible Methodology for Decontamination of EA 2192, the Toxic Byproduct of VX Hydrolysis. *Inorg. Chem*. **2011,** *50* (7), 3071–3077.

48. Andrea, T.; Neverov, A.A., Brown, R.S. Efficient Methanolytic Cleavage of Phosphate, Phosphonate, and Phosphonothioate Ester Promoted by Solid Supported Lanthanide Ions. *Ind. Eng. Chem. Res.* **2010,** *49* (15), 7027–7033.

49. Evans, R.A.; Smith, W.L.; Nguyen, N.P.; Crouse, K.L.; Norman, S.D.; Jakubowski, E.M. Quantification of VX Vapor in Ambient Air by Liquid Chromatography Isotope Dilution Tandem Mass Spectrometric Analysis of Glass Bead Filled Sampling Tubes. *Anal. Chem.* **2011,** *83* (1), 1315–1320.

50. Prokofieva, D.S.; Voitenko, N.G.; Gustyleva, L.K.; Babakov, V.N.; Savelieva, E.I.; Jenkins, R.O.; Goncharov, N.V. Microplate Spectroscopic Methods for Determination of the Organophosphate Soman. *J. Environ. Monit.* **2010,** *12,* 1349–1354.

Blank

ACRONYMS AND ABBREVIATIONS

$(Bu_4N^+)F^-$	tetrabutylammonium fluoride
CARC	chemical agent-resistant coating
CAS	Chemical Abstracts Service
CASARM	chemical agent standard analytical reference material
CH_3O^-	methoxide ion
CWA	chemical warfare agent
CWC	Chemical Weapons Convention
ECBC	U.S. Army Edgewood Chemical Biological Center
$\Delta G^{\ddagger}$	change in Gibbs free energy
$\Delta H^{\ddagger}$	change in enthalpy
$\Delta S^{\ddagger}$	change in entropy
DS2	decontamination solution 2
GA	tabun
GB	sarin
GC-MS	gas chromatography–mass spectrometry
GD	soman
GF	cyclosarin
HD	sulfur mustard
k_2	second-order rate constant
k_2^{obs}	observed second-order rate constant
k_{cat}	rate constant
K_m	Michaelis constant
k_{obs}	observed first-order rate constant
K_{OC} (log)	carbon partition coefficient
K_{OW} (log)	octanol/water partition coefficient
$La(OTf)_3$	lanthanum trifluoromethanesulfonate
LC-MS	liquid chromatography–mass spectrometry
LD_{50}	dose that is lethal to 50% of test subjects
MICA	metal ion-catalyzed alcoholysis
NATO	North Atlantic Treaty Organization
NMR	nuclear magnetic resonance
OP	organophosphorus
OPIDN	organophosphorus ester-induced delayed neuropathy
^{31}P NMR	phosphorus-31 nuclear magnetic resonance spectroscopy
$^{s}_{s}pH$	negative logarithm of the pH in specified solvent
pKa	acid dissociation constant
$^{s}_{s}pK_a$	negative logarithm of the equilibrium constant for association
PTE	phosphotriesterase
RAJEP	Russian–American Joint Evaluation Program
RD4M	Russian reactive decontaminant 4, modified

RIHOPHE	Research Institute of Hygiene, Occupational Pathology, and Human Ecology
RV-bis	phosphonodithioic acid; methyl-*S*,*S*-bis[diethylamino ethyl] ester
RVX	Russian *O*-(2-methylpropyl)-*S*-(2-diethylaminoethyl) methylphosphonothioate
$Sm(OTf)_3$	samarium trifluoromethanesulfonate
$t_{1/2}$	half-life
TNO	Netherlands Organisation for Applied Scientific Research
USVX	U.S. *O*-ethyl-*S*-(2-diisopropylaminoethyl) methylphosphonothioate
UV-vis	ultraviolet–visible

DISTRIBUTION LIST

The following individuals and organizations were provided with one Adobe portable document format (pdf) electronic version of this report:

U.S. Army Edgewood Chemical
Biological Center (ECBC)
RDCB-DRC
ATTN: Berg, F.

ECBC Technical Library
RDCB-DRB-BL
ATTN: Foppiano, S.
Stein, J.

Defense Threat Reduction Agency
J9-CBS
ATTN: Peacock-Clark, S.
Cronce, D.

Office of the Chief Counsel
AMSRD-CC
ATTN: Upchurch, V.

Defense Technical Information Center
ATTN: DTIC OA

Department of Homeland Security
RDCB-PI-CSAC
ATTN: Mearns, H.

ECBC Rock Island
RDCB-DES
ATTN: Lee, K.
RDCB-DEM
ATTN: Grodecki, J.

G-3 History Office
U.S. Army RDECOM
ATTN: Smart, J.


EDGEWOOD CHEMICAL BIOLOGICAL CENTER
A U.S. Army RDECOM Laboratory